R-06-16

Rock mechanics modelling of rock mass properties – theoretical approach

Preliminary site description

Laxemar subarea – version 1.2

Anders Fredriksson, Isabelle Olofsson
Golder Associates AB

June 2007

Svensk Kärnbränslehantering AB
Swedish Nuclear Fuel
and Waste Management Co
Box 5864
SE-102 40 Stockholm Sweden
Tel 08-459 84 00
+46 8 459 84 00
Fax 08-661 57 19
+46 8 661 57 19

ISSN 1402-3091
SKB Rapport R-06-16

Rock mechanics modelling of rock mass properties – theoretical approach

Preliminary site description

Laxemar subarea – version 1.2

Anders Fredriksson, Isabelle Olofsson
Golder Associates AB

June 2007

This report concerns a study which was conducted for SKB. The conclusions and viewpoints presented in the report are those of the authors and do not necessarily coincide with those of the client.

A pdf version of this document can be downloaded from www.skb.se.

Symbols and abbreviations

c_i	Cohesion of intact rock [MPa]
c_f	Peak cohesion of fracture [MPa]
c_m	Peak cohesion of the rock mass, Mohr-Coulomb [MPa]
D	Density [kg/m^3]
epsh	Horizontal strain
epsv	Vertical strain
epsx	Strain in the X direction (horizontal)
epsy	Strain in the Y direction (vertical)
epsz	Strain in the Z direction
E_i	Young's modulus of the intact rock [GPa]
E_m	Young's modulus of the rock mass [GPa]
GSI	Geological Strength Index
j_r	Material parameter for joint roughness [m]
K_n	Joint normal stiffness at expected normal stress [MPa/m]
K_s	Joint shear stiffness at expected normal stress [MPa/m]
k_r	Exponent in Power Law size distribution
m_i	Material constant in Hoek-Brown criterion for intact rock
$\Delta\sigma_y$	Increment in stress along y-axis [MPa]
ε_x	Strain in the X direction (horizontal)
ε_y	Strain in the Y direction (vertical)
φ_i	Internal friction angle of intact rock [°]
φ_f	Internal friction angle of fracture, Mohe-Coulomb [°]
φ_m	Internal friction angle of rock mass[°]
ν_i	Poisson's ratio of the intact rock
σ_c	Uniaxial compressive strength, Hoek&Brown [MPa]
ν_m	Poisson's ratio of the rock mass
σ_t	Tensile strength, Hoek&Brown [MPa]
σ_{vf}	Vertical stress at failure [MPa]
T_i	Tensile strength of intact rock[MPa]
UCS_i	Uniaxial compressive strength of intact rock [MPa]
UCS_m	Uniaxial compressive strength of rock mass [MPa]
X_{r0}	Minimum radius in Power Law size distribution

Abstract

The present report summarises the theoretical approach to estimate the mechanical properties of the rock mass in relation to the Preliminary Site Descriptive Modelling, version 1.2 Oskarshamn, Laxemar subarea.

The theoretical approach is based on a discrete fracture network (DFN) description of the fractured rock mass system and on the results of mechanical testing of intact rock and on rock fractures.

To estimate the mechanical properties of the rock mass a load test on a rock block with fractures was simulated with the numerical code 3DEC. Fracture network realisations were first generated with the numerical software FracMan, which were then transferred into the mechanical model. The rock block was loaded in plain strain condition. From the calculated relationship between stresses and deformations the mechanical properties of the rock mass were determined.

The influence of the geometrical properties of the fracture system on the mechanical properties of the rock mass was analysed by loading 20 blocks based on different DFN-realisations. The material properties of the intact rock and the fractures were kept constant. The properties were set equal to the mean value of each measured material property.

The influence that variability in mechanical properties of intact rock and fractures may have on the rock mass were not analysed during this step. The main interests were focused on the influence of the fracture intensity and stochastic DFN geometry on the rock mass properties.

Sammanfattning

Denna rapport sammanfattar det teoretiska angreppssättet att uppskatta bergmassans mekaniska egenskaper i samband med den Platsbeskrivande modellen version 1.2 för Oskarshamn, delområde Laxemar.

Det teoretiska angreppssättet baseras dels på en geometrisk DFN-beskrivning av bergmassans spricksystem och dels mekaniska laboratorietester utförda på intakt berg och på bergsprickor.

För att uppskatta bergmassans mekaniska egenskaper utfördes ett numeriskt belastningsförsök på ett bergblock i den numeriska koden 3DEC. Läge och storlek på sprickorna i blocket baseras på DFN-realiseringar. Blocket belastades under plant töjningstillstånd.

Inverkan av spricksystemets geometriska utformning bestämdes genom att analysera ca 20 stycken DFN-realiseringar med konstanta egenskaper hos det intakta berget och hos sprickorna. Egenskaperna sattes lika med de uppmätta medelvärdena för respektive egenskap.

Inverkan av det intakta bergets och sprickornas mekaniska egenskaper studerades inte i detta steg utan fokus koncentrerades på inverkan av sprickintensitet på bergmassans mekaniska egenskaper.

Contents

1 Introduction

This work reports results from one of the four rock mechanics activities that have been recognised within the project "Oskarshamn – Site Descriptive Model during the initial Site Investigation stage version 1.2". This activity aims to determine the undisturbed mechanical properties of the rock mass in the local model for subarea Laxemar 1.2. These parameters will be distributed to the "Design team", who will evaluate the suitability of the site.

The approach in this activity was based on numerical simulations with the 3DEC software. The methodology was developed for the purpose of the Site Investigations and it was built upon two different models: i) the DFN model, which is used to generate fracture network realisations of the rock mass, and ii) the 3DEC mechanical model, which is used to calculate the rock mass mechanical properties. This modelling procedure is described in more detail in /Olofsson and Fredriksson 2005/ and has earlier been used for the Oskarshamn 1.2 Simpevarp area Rock mechanics site descriptive model /Fredriksson and Olofsson 2005/.

The work was conducted according to the Activity Plan for "Establishment of a site descriptive model for the rock mechanics description of the Laxemar subarea (version 1.2)". According to this Activity Plan the theoretical model should focus on the influence of fracture intensity on the properties of the rock mass.

The DFN model, the in situ stresses as well as the mechanical properties of intact rock and fractures constitute the input data that are necessary to build the 3DEC model. The set-up of the 3DEC model, the procedure used for numerical simulations and the results obtained are described in the following.

2 Indata

2.1 Intact rock

The mechanical properties of the intact rock are presented in Table 2-1 and the ground for their evaluation is presented in /Lanaro et al. 2006/.

Table 2-2 presents the lithological description of the rock domain A, which was required to know what parameters of the intact rock needed to be inserted in the numerical model. One rock type, granite to granodiorite, is strongly dominant, and the intact rock parameters for this rock type were used for numerical modelling.

Table 2-1. Measured rock mechanical properties for intact rock (matrix) for two rock types (i.e. small pieces of rock without any fractures).

Parameter for intact rock (drill core scale)	Fine-grained dioritoid (metavolcanite, vulcanite)	Quartz monzonite to monzodiorite	Granite to quartz monozodiorite (Ävrö granite)	Sealed fractures in intact rock
Uniaxial compressive strength, UCS_i, Mean/standard dev.	205 [MPa]/51 [MPa]	161 [MPa]/24 [MPa]	192 [MPa]/21 [MPa]	126 [MPa]/31 [MPa]
UCS_i Min trunc – Max trunc	109–264 [MPa]	118–193 [MPa]	151–239 [MPa]	92–158 [MPa]
Young's modulus, E_i, Mean/standard dev.	85 [GPa]/7 [GPa]	78 [GPa]/7 [GPa]	72 [GPa]/5 GPa]	91 [GPa]/10 [GPa]
E_i, Min trunc – Max trunc	78–101 [GPa]	69–86 [GPa]	61–89 [GPa]	83–104 [GPa]
Poisson's ratio, ν_i, Mean/standard dev.	0.26/0.03	0.27/0.05	0.20/0.03	0.24/0.07
ν_i, Min trunc – Max trunc	0.21–0.31	0.19–0.33	0.15–0.26	0.18–0.31
Tensile strength, T_i, Mean/standard dev.	19 [MPa]/2[MPa]	18 [MPa]/4 [MPa]	13.0 [MPa]/1.5 [MPa]	14 [MPa]/5[MPa]
T_i, Min trunc – Max trunc	14–24 [MPa]	12–24 [MPa]	9.3–16.4 [MPa]	9–22 [MPa]
Mohr – Coulomb, ϕ_i, Mean/standard dev.	52.7[°]/ 0.6 [°]	59.5[°]/ 0.4 [°]	55.9 [°]/0.3 [°]	52.3[°]/1.1 [°]
ϕ_i, Min trunc – Max trunc	51.2 [°]–53.5 [°]	58.7 [°]–60.1 [°]	53.5 [°]–57.1 [°]	49.3 [°]–53.7 [°]
Mohr – Coulomb, c_i, Mean/standard dev.	33.0 [MPa]/7.1[MPa]	20.3 [MPa]/2.0 [MPa]	27.4 [MPa]/2.5 [MPa]	19.2 [MPa]/4.8 [MPa]
c_i, Min trunc – Max trunc	19.3–47.1 [MPa]	16.5–24.3 [MPa]	23.2–32.3 [MPa]	20.1–29 [MPa]

Table 2-2. Rock types in the simulated rock domain A.

	Main rock type	%	Subordinate rock types	%
RSMA01	Ävrö granite	54–92	Fine- to medium-grained granite	1–22
			Pegmatite	0–1
			Fine-grained dioritoid	2–21
			Diorite to gabbro	0–12
			Fine-grained diorite to gabbro	0–5
			Quartz monzodiorite	1–14

2.2 Fractures

2.2.1 Geometry of fractures

The fracture geometry parameters used in this modelling approach were taken from the DFN model of Laxemar version 1.2 that was delivered and presented on the 20th April 2005 and is reported by /Hermanson et al. 2005/. It should be emphasised that this DFN model was not the final version, but at the time scheduled for the Rock Mechanics model the statistical parameters of the DFN model comprised the best available understanding of fracture geometry. Therefore, the parameters given during the meeting on the 20th April 2005 were used for most of the simulations in this study. The DFN model version 1.2 covers both the Laxemar and the Simpevarp subareas.

The DFN model for both the Laxemar and the Simpevarp subareas share the following definitions:

1. Fractures sets that are 'regional' in scope (i.e. follow a power-law scaling relationship between outcrop-scale and lineament-scale, and are seen in both subareas) are labelled using capitalized letter (A, B, C).
2. Fracture sets that are 'local' in scope (i.e. their distribution is confined to a single subarea) are labelled using lower-case letters (d,e,f).
3. Both the Laxemar and Simpevarp subareas feature a fracture set consisting of primarily subhorizontal fractures. To avoid confusion, this set is defined as 'Set d' in both subareas, even through the actual set properties vary between modelling subareas.

The DFN model parameters for Laxemar subarea that were used for generating 3D fracture network realisations for the mechanical model are presented below.

Orientation

The trend and plunge of each fracture set mean pole, and the dispersion around the mean poles are given for each set in Table 2-3. The fracture sets definitions are based on all fractures observed (i.e. disregarding whether fractures are defined as open, partly open or sealed according to BOREMAP mapping). The local fracture set S_e exists only in the Simpevarp subarea, and was therefore not considered in this study.

Size distribution

The size distribution used is the one provided in the DFN model version 1.2 and the parameters are given in Table 2-4. In the initial simulations, a power-law model was used for fracture set S_d although an exponential model gives a better fit.

Table 2-3. Orientation of all fracture sets in the Laxemar subarea.

Set	Best model	Mean pole trend [°]	Mean pole plunge [°]	Dispersion
S_A	Univ.Fisher	338.1	4.5	k=13.06
S_B	Univ.Fisher	100.4	0.2	k=19.62
S_C	Univ.Fisher	212.9	0.9	k=10.46
S_d	Univ.Fisher	3.3	62.1	k=10.13
S_f	Univ.Fisher	243.0	24.4	k=23.51

Table 2-4. Size distribution for all fracture sets in Laxemar subarea.

Set	Size distribution model	Power law (Parent radius distribution)	
		Exponent, k_r	Minimum radius, X_{r0}, m
S_A	Power law	3.18	0.716
S_B	Power law	3.04	2.2627
S_C	Power law	3.0	1.676
S_d	Power law	2.9	0.208
	Exponential [1]	0.25	
S_f	Power law	3.6	0.4

(1) An exponential size distribution provides the best fit for S_d. Nevertheless, in the initial simulations the power law was used for S_d. Data for the power law were also given by /Hermanson et al. 2005/.

Intensity

The fracture intensity that is used for the rock mechanics model is based on fracture frequency data from boreholes and calibrated for modelling scales in the range 30–100 metres. Table 2-5 presents the fracture intensity in terms of P_{32} values, which is defined by fracture area per rock volume, and standard deviation.

For the simulations only open fractures with a radius from 0.5 m up to 100 m were generated in the DFN realisations. Therefore, the P_{32} values used for the mechanical model need to be adjusted for the particular truncation of fracture radii. The P_{32} values were adjusted according to the method given by /Hermanson et al. 2005/. Furthermore, three cases of fracture intensity were selected for modelling mechanical rock mass properties: $P_{32\ low}$, which is the adjusted mean P_{32} minus one standard deviation, $P_{32\ mean}$, which is simply the adjusted mean fracture intensity, and $P_{32\ high}$, which is the adjusted mean P_{32} plus one standard deviation. These cases are shown in Table 2-6.

Table 2-5. P_{32} for all fracture sets in the rock domain RSMA01 in Laxemar subarea.

Set	P_{32} All		Open percentage	P_{32} Open	
	Mean	Std. Dev.		Mean	Std. Dev
S_A	1.43	0.73	42.48	0.61	0.31
S_B	1.69	1.34	37.85	0.64	0.51
S_C	1.52	1.23	41.25	0.63	0.51
S_d	2.32	1.58	40.10	0.93	0.63
S_f	1.40	1.15	42.05	0.59	0.48

Table 2-6. Three cases of adjusted P_{32} used in the mechanical model. The P_{32} are adjusted for truncation of the fracture radius distribution (0.5–100.0 m) in the rock domain RSMA01 in Laxemar subarea.

Set	$P_{32\ low}$	$P_{32\ mean}$	$P_{32\ high}$
S_A	0.30	0.61	0.91
S_B	0.13	0.63	1.12
S_C	0.12	0.62	1.12
S_d	0.13	0.42	0.70
	0.20[1]	0.63[1]	1.06[1]
S_f	0.07	0.41	0.75

[1] Exponential size distribution.

2.2.2 Mechanical properties of fractures

Laboratory normal load tests up to 10 MPa and shear tests have been performed on fractures at normal stress levels of 0.5, 5 and 20 MPa from boreholes KSH01, KSH02, KAV01, KLX02, and KLX04. The laboratory tests were evaluated and the results are given in /Lanaro et al. 2006/.

The data was analysed statistically and it was considered reasonable to approximate the data by truncated normal distributions /see Lanaro et al. 2006/. Statistical inference tests were also used to examine if fracture properties differ significantly between fracture sets. In essence, the differences between the different fracture sets were found to be of minor relevance, in relation to uncertainties associated with the laboratory test methods /Lanaro et al. 2006/. Therefore the mechanical properties were determined to be equal for all fracture sets. The preliminary mechanical properties of fractures, in terms of mean, standard deviation, upper and lower truncation limit for each parameter, that were available at this stage are presented in Table 2-7.

2.3 In situ stresses

Two different stress domains were defined in Simpevarp and Laxemar subareas /Hakami and Min 2005/. Their state of stress was simulated in a numerical model to give representative in situ stresses at 500m depth /Table 2-8/. The stresses differ in magnitude between the two different stress domains but their orientation is similar. Based on the given in situ stresses at 500 m depth the following three different confining stress levels have been used in the simulations: 32 MPa, 8 MPa and 0.5 MPa. The results of the simulations are then valid for both stress domains.

Table 2-7. Summary of mechanical properties of fractures evaluated from laboratory tests.

Parameter for single fractures (small scale)	All fracture sets Truncated normal distribution Mean/Standard deviation;	Min trunc. – Max trunc.
Normal stiffness, K_n	221.9/42.6 [MPa/mm]	150.1–305.3 [MPa/mm]
Shear stiffness, K_s	41.37/11.6 [MPa/mm]	18.3–66.6 [MPa/mm]
Peak friction angle, ϕ_f	36.6/3.01 [°]	31.18–40.83 [°]
Cohesion, c_f	0.82/0.37 [MPa]	0.26–1.56 [MPa]

Table 2-8. In situ stress magnitude and orientation for both stress domains at 500 m depth (from /Hakami and Min 2005/).

	Stress domain I			Stress domain II		
	σ_1	σ_2	σ_3	σ_1	σ_2	σ_3
Mean magnitude, MPa	32	14	9.5	16	9	5.5
Mean strike, °	132	90	42	132	90	42
Mean dip, °	0	90	0	0	90	0

3 Set-up of the model

3.1 Description of the numerical simulations

The parameters presented in section 2.2.1 were used to generate the 3D fracture network realisations that were transferred into the 3DEC software.

Three sets of fracture network realisations with different fracture intensities were generated for rock domain RSMA01. For each set, 20 realisations of the same fracture network were generated in a cubic domain (side length 40 m). The dimensions of the cube are chosen to be much larger than the rock block modelled in 3DEC (side length 20 m) to avoid truncation effects at the boundaries. The first set or realisation was assigned a low fracture intensity (P_{32} = mean value – one standard deviation), the second set had a mean fracture intensity (P_{32} = mean) and the third had a high fracture intensity (P_{32} = mean value + one standard deviation) (see Table 2-6). Based on the results of laboratory tests, the assumption was made that sealed fractures do not significantly influence the mechanical behaviour of the rock mass. Therefore, only open and partly open fractures were included in the DFN model.

The vertical fracture frequency, P_{10} values (number of fractures per meter), was sampled in each realisation, using nine vertical boreholes evenly distributed in the box. The mean value of the P_{10} in the boreholes was calculated and saved as a measure of the P_{10} for that realisation.

Next, 2D vertical sampling planes, parallel to the maximum principal stress (σ_1), were used to extract fractures from each 3D fracture network realisation. The trace data in these planes were used for input in 3DEC. The identification of each fracture set was maintained throughout the process to allow different mechanical properties to be assigned to the different fracture sets.

Three examples of extracted fracture trace planes are given in Figure 3-1, Figure 3-2, and Figure 3-3; the traces have been extracted from 3D DFN realisations with different fracture intensity: P_{32} low, P_{32} mean, and P_{32} high, respectively.

Figure 3-4 shows the corresponding 3DEC model for the realisation with low fracture intensity (i.e. Figure 3-1). Each fracture in the 3DEC model is divided in a number of contact points. Each contact point corresponds to an area of the fracture depending on the zone size given. As an example, the contact points along each fracture in the 3DEC model (Figure 3-4) are shown in Figure 3-5.

When the rock block model is built it is first consolidated for the confining effective stress (32 MPa, 8 MPa or 0.5 MPa) then loaded in the vertical direction with constant rate of deformation.[1]

The result in the form of vertical stress-vertical strain and horizontal strain–vertical strain curves from one simulation with 3DEC is shown in Figure 3-6.

The deformation modulus, E_m and Poisson's ratio, ν_m, of the rock mass were evaluated from vertical stress – vertical strain and horizontal strain – vertical strain curves. The strength parameters of the rock mass, uniaxial strength, UCS_m, cohesion, c_m, and friction, φ_m, were evaluated from simulations with different confining stress. The following equations were used:

$$\phi_m = \arcsin\left(\frac{k-1}{k+1}\right) \quad (2.1)$$

$$UCSm = \sigma_{1b} + k \cdot \sigma_{3b} \quad (2.2)$$

[1] The confining stress applied to the model is assumed equal to the effective confining stress despite the fact that the fracture samples tested are dried and with no pore pressure. There is no indication that the fracture mechanical properties would be the same in case of water saturated tests.

$$c_m = UCS_m \cdot (1-\sin\phi_m)/2\cdot\cos\phi_m \quad (2.3)$$

where $k = (\sigma_{1a}-\sigma_{1b})/(\sigma_{3a}-\sigma_{3b})$ and σ_{1a}, σ_{1b}, σ_{3a} and σ_{3b} are the principal stresses at failure at two confining stresses a and b.

The procedure is described in more detail in /Olofsson and Fredriksson 2005/.

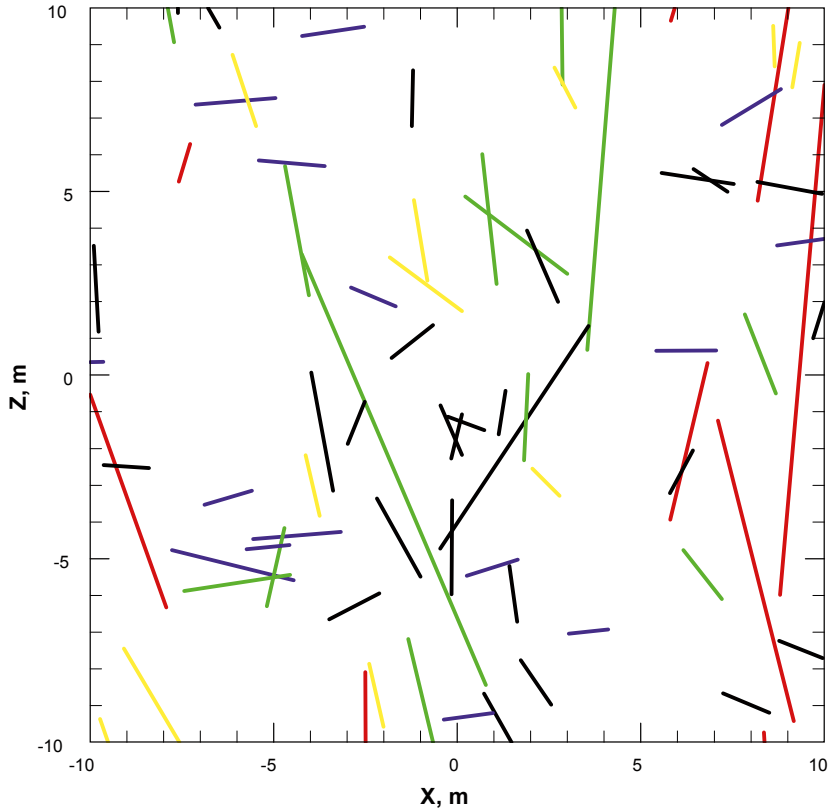

Figure 3-1. *Example of fracture traces in a vertical plane when P_{32} is low. Fracture traces of different fracture sets have different colours.*

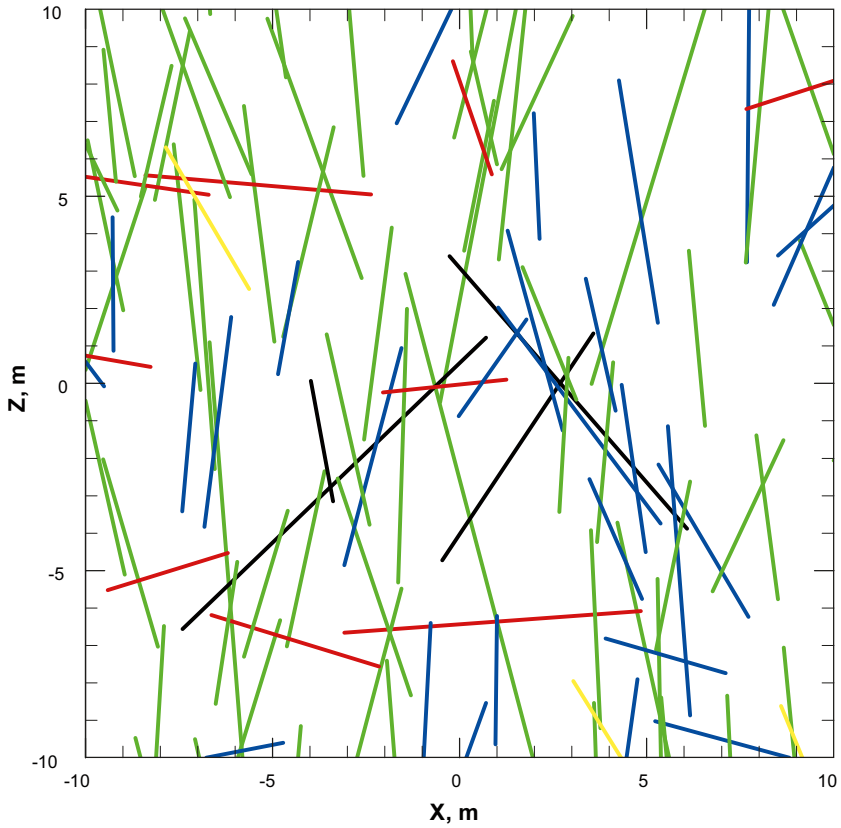

Figure 3-2. *Example of fracture traces in a vertical plane. P_{32} is equal to its mean value. Fracture traces of different fracture sets have different colours.*

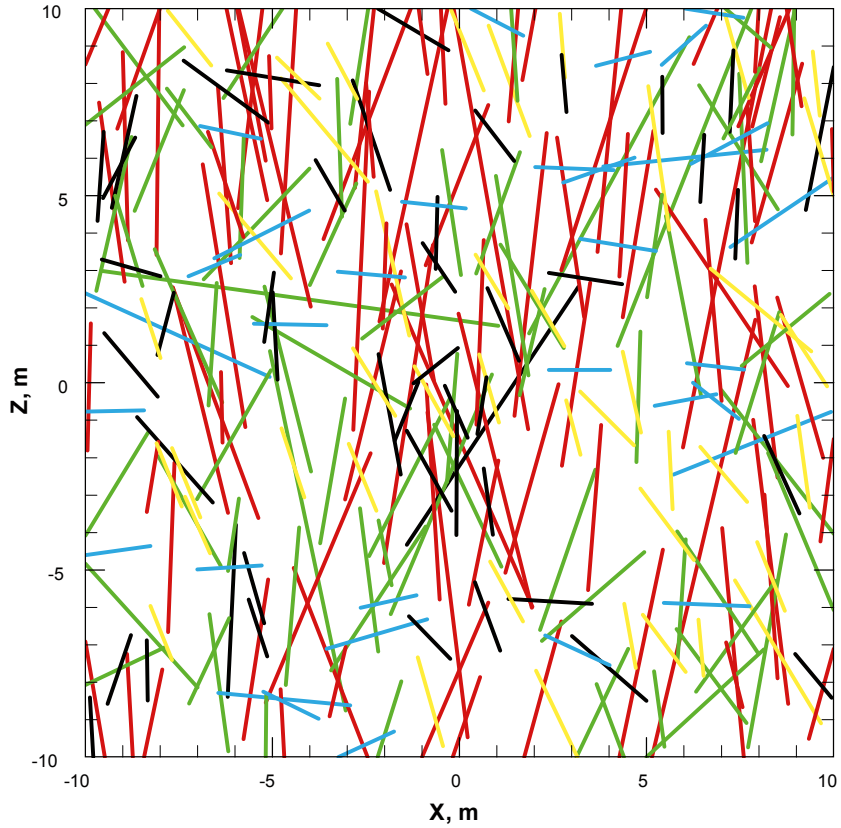

Figure 3-3. *Example of fracture traces in a vertical plan when P_{32} is high. Fracture traces of different fracture sets have different colours.*

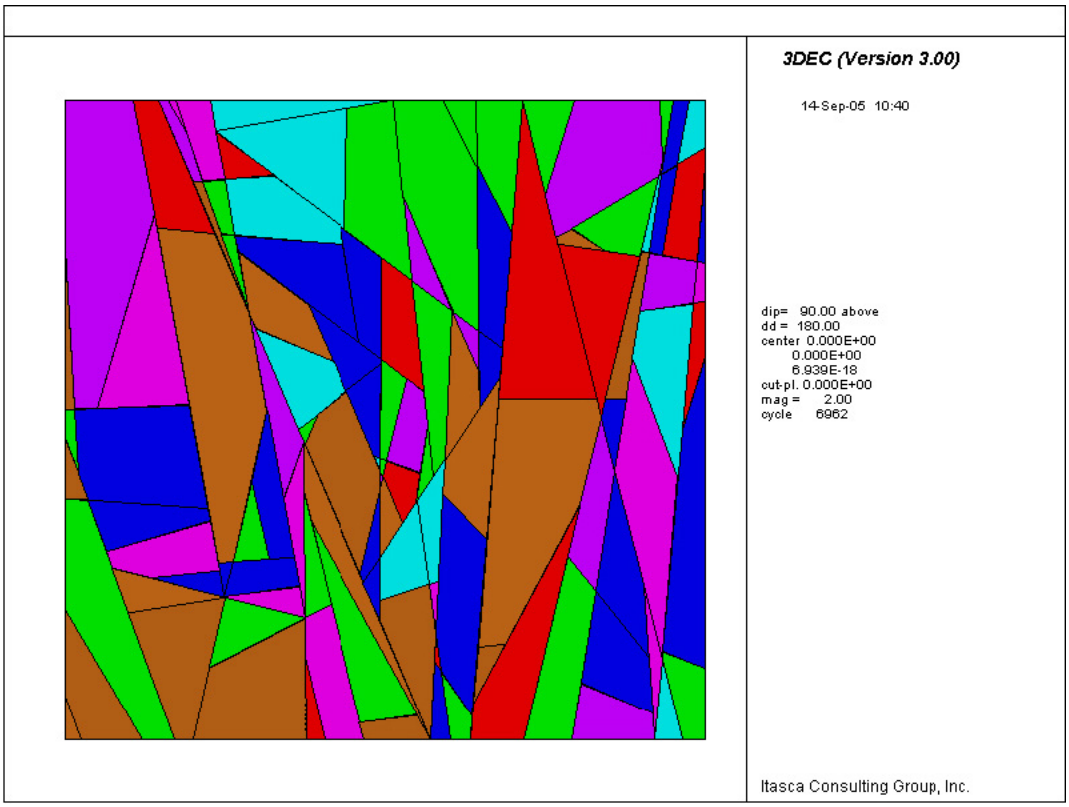

Figure 3-4. *3DEC model generated from the example of fracture traces with low P_{32}, shown in Figure 3-1.*

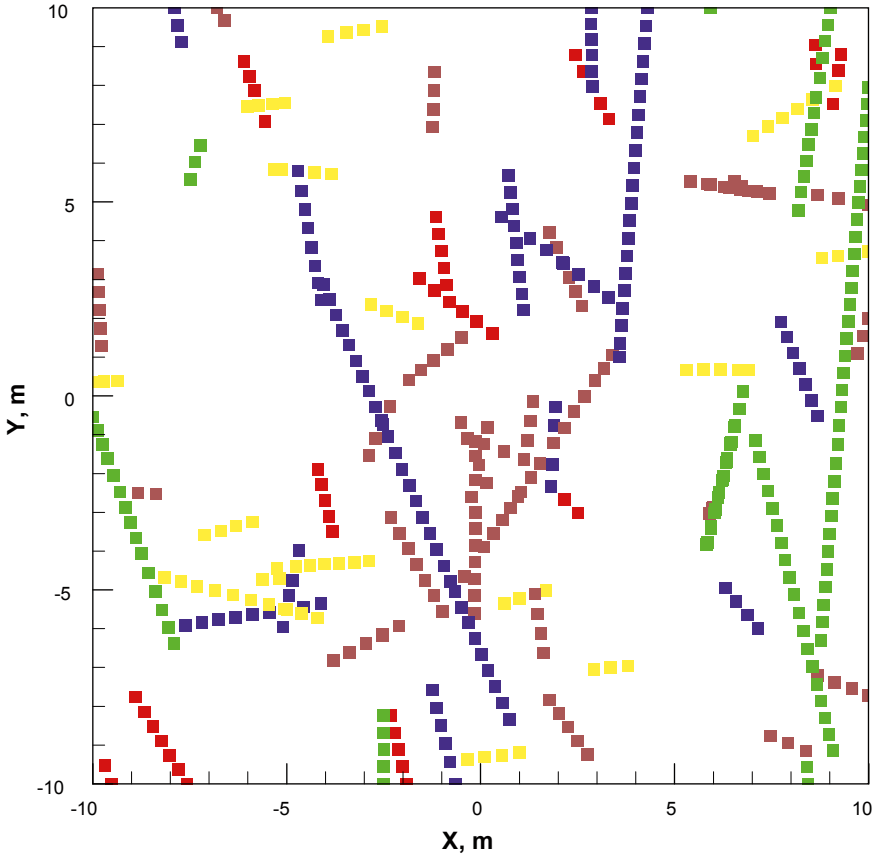

Figure 3-5. *Active contact points along fractures in the 3DEC model.*

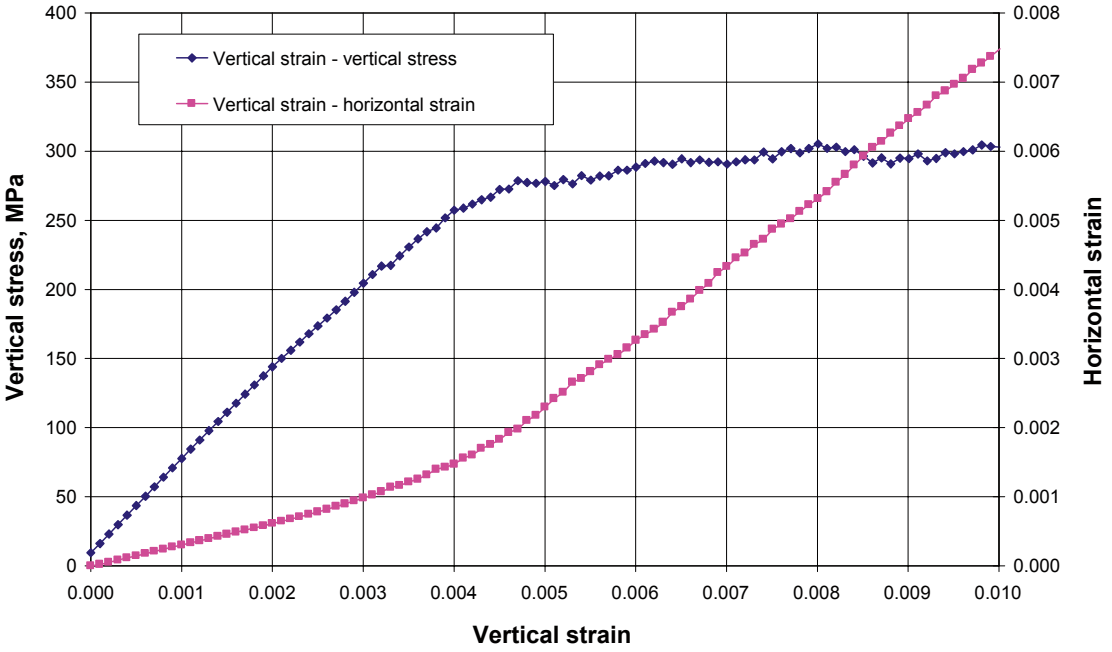

Figure 3-6. *Example of stress-strain curves.*

3.2 Estimation of uncertainty

The uncertainty of a model can be separated into conceptual uncertainty, data uncertainty and spatial variability. The conceptual uncertainty originates from an incomplete understanding of the principal structure of the analyzed system and its interacting processes. This uncertainty is not further discussed.

Data uncertainty concerns the uncertainty in parameter values being used in a model; it may be caused by measuring errors, interpretation errors or uncertainty in extrapolation of spatially variable parameters.

Spatial variability concerns the variation in space of a parameter value; although this is not strictly an uncertainty, in combination with practical limitations in rock characterization, it constitutes an indirect source for data uncertainty. Hence, in the following, no distinction is made to what extent the estimated rock mass parameter distributions relate to spatial variability and/or data uncertainty.

In the case of the present data, stochastic material properties of intact rock and of fractures are approximated by empirical, truncated, normal distributions that are defined by their mean, standard deviation, minimum and maximum values. Likewise, the DFN geometry is given as stochastic distributions.

Ideally, rock mass property distributions could be estimated by iterative 3DEC simulations involving numerous stochastic DFN realisations, where the DFN geometry and material property parameters are allowed to take any value from their defined input distributions. However, such a direct approach becomes impractical due to its computational demand and limitations in parameter descriptions in 3DEC.

Instead, a simplified stochastic approach was used. Here, 3DEC was only used to estimate the DFN geometry-induced variability on rock mass properties as outlined in the Activity Plan. The properties of the intact rock and the fractures were assigned their mean values and kept constant.

4 Simulations with different fracture intensity in the DFN model

4.1 Input material data

The mean material parameters for the intact rock and the fractures used in the simulations are given in Table 4-1. The modulus of the intact rock was reduced to 90% of the value determined on laboratory samples due to scale effects. The parameters for the intact rock differ anyway from those given in Table 2-1 because the values in Table 4-1 are based on an early evaluation of the parameters for intact rock. The values are still in the span of variation of the mean value for the different parameters. Previous sensitivity analyses on the impact of the input parameters on the modelled rock mass properties have been conducted for Simpevarp v 1.2 /Fredriksson and Olofsson 2005/. Assuming that the results of this study also applies to Laxemar (considering that also the fracture network is different), the deformation modulus and Poisson's ratio of the rock mass simulated with parameters given in Table 4-1 will be slightly higher than the if the mean value of these parameters as given in Table 2-1 had been used as there are positively correlated to the intact rock deformation modulus. Nevertheless these are not expected to have a large and significant influence on the modelled rock mass properties.

Table 4-1. Input parameter for intact rock and fractures.

		Mean
Intact rock, RSMA01	E_i [GPa]	69
	ν_i [–]	0.23
	ϕ_i [°]	51.4
	c_i [MPa]	33.96
	T_i [MPa]	17.0
Fractures	K_n [MPa/mm]	221.9
	K_s [MPa/mm]	41.4
	ϕ_f [°]	36.6
	c_f [MPa]	0.82

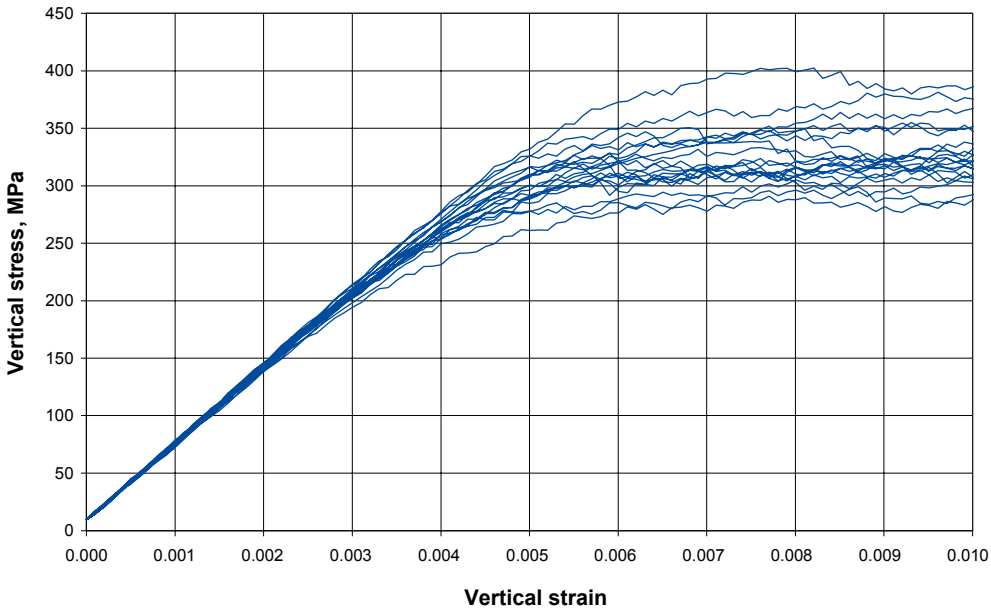

Figure 4-1. *Calculated stress-strain curves with 3DEC for one set of DFN realisations.*

4.2 DFN geometry-induced variability in rock mass strength and deformability

These simulations were run in order to quantify the influence of the fracture pattern and different levels of fracture intensity (P_{32}) on the rock mass mechanical parameters. This was achieved by running three sets of DFN realisations with different fracture intensity in 3DEC, while all mechanical parameters were kept constant. Each of the three sets contained 20 realisations of the same DFN model (i.e. Monte Carlo simulations with P_{32} constant). Calculated stress-strain curves are shown in Figure 4-1 for one set of DFN realisations. The statistical parameters used for simulating the DFN model are listed in Table 2-3 to Table 2-6.

Each DFN realisation set was analysed at three different effective stress levels, 32 MPa (equivalent to the maximum principal stress σ_1), 8.0 MPa (25% of σ_1) and 0.5 MPa. The mechanical models were loaded with a constant velocity in the vertical direction while the horizontal stresses were constant during the loading test. The deformation modulus, E_m, Poisson's ratio, ν_m, and the vertical stress at failure, σ_{vf}, were evaluated at the three stress levels to provide an estimation of φ_m and c_m. The stress at failure, σ_{vf}, is defined as, either the maximum vertical stress, or the vertical stress at 0.010 vertical strain if the vertical stress – vertical strain curve does not show a marked maximum.

The mean values of intact rock properties and fracture properties were used in the simulations (as given in Table 4-1).

The evaluated rock mass parameters, E_m and ν_m at 32 MPa, 8.0 MPa and 0.5 MPa for each realisation are presented in Appendix A Tables A-1, A-2 and A-3 for P_{32} low, in Appendix B Tables B-1, B-2 and B-3 for P_{32} mean and in Appendix C Tables C-1, C-2 and C-3 for P_{32} high.

The obtained distributions for $E_{m\,(32\ MPa)}$, $\nu_{m\,(32\ MPa)}$, $E_{m\,(8.0\ MPa)}$, $\nu_{m\,(8.0\ MPa)}$, $E_{m\,(0.5\ MPa)}$, and $\nu_{m\ (0.5\ MPa)}$ are summarized in Table 4-2 for Rock Domain RSMA01. It should be noted that the variability of parameters in Table 4-2 only accounts for the influence that a stochastic fracture pattern and different fracture intensity have on the rock mass properties (as all mechanical input parameters are kept constant).

Using the RocData software /RocData 2004/ a linear Mohr–Coulomb failure envelope and a non-linear Hoek-Brown envelope were fitted to the three Mohr circles obtained at failure. The Hoek-Brown envelope was fitted by adjusting the GSI value and the m_i value until the envelope touched the Mohr circles. An example of a fitted non-linear Hoek-Brown envelope is shown in Figure 4-2. The notations H&B and MC are used to distinguish between the Hoek-Brown and Mohr–Coulomb model parameters.

The evaluated cohesion (c_m MC), friction angle (φ_m MC), GSI value, m_i value, tensile strength (σ_t H&B) and uniaxial compressive strength (σ_c H&B) of the rock mass for each realisation are presented in Appendix A Table A-4, Appendix B Table B-4 and Appendix C Table C-4.

The obtained distributions for the strength parameters GSI, m_i, σ_t H&B, σ_c H&B, c_m MC and φ_m MC are summarized in Table 4-3 for Rock Domain RSMA01. The parameters that are given in this table only account for the influence of the variation in the fracture pattern and intensity on the rock mass properties (as input mechanical parameters are constant)

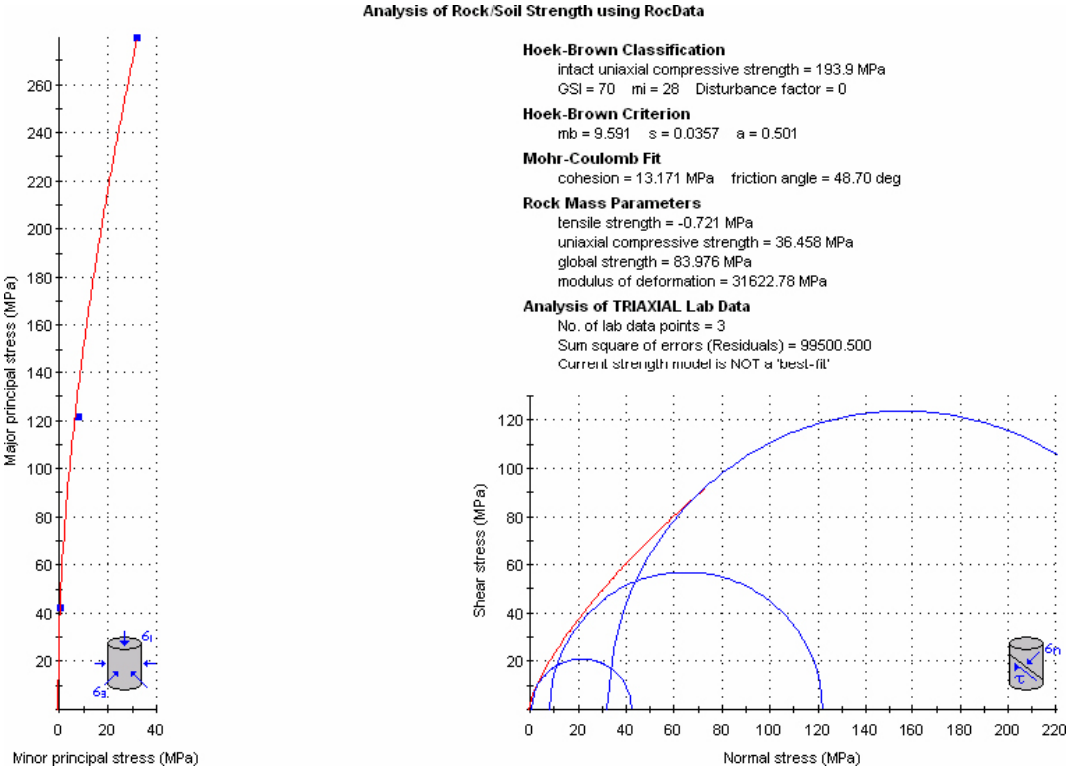

Figure 4-2. *Fitted Hoek-Brown envelope to the three Mohr circles.*

Table 4-2. DFN geometry-induced variability in rock mass deformation properties of Rock Domain RSMA01.

Variable	P_{32}	Mean	Std. Dev.	Min.	Max.
$E_{m\ (32\ MPa)}$	Low	62.90 GPa	1.17 GPa	60.92 GPa	64.80 GPa
$v_{m\ (32\ MPa)}$	Low	0.24	0.003	0.23	0.24
$E_{m\ (8\ MPa)}$	Low	61.73 GPa	2.37 GPa	55.91 GPa	64.94 GPa
$v_{m\ (8\ MPa)}$	Low	0.24	0.1	0.23	0.28
$E_{m\ (0.5\ MPa)}$	Low	54.73 GPa	6.11 GPa	39.83 GPa	63.12 GPa
$v_{m\ (0.5\ MPa)}$	Low	0.29	0.05	0.23	0.37
$E_{m\ (32\ MPa)}$	Mean	54.78 GPa	1.81 GPa	51.47 GPa	57.13 GPa
$v_{m\ (32\ MPa)}$	Mean	0.25	0.003	0.25	0.26
$E_{m\ (8\ MPa)}$	Mean	52.31 GPa	2.31 GPa	47.97 GPa	56.57 GPa
$v_{m\ (8\ MPa)}$	Mean	0.27	0.01	0.25	0.29
$E_{m\ (0.5\ MPa)}$	Mean	41.94 GPa	8.59 GPa	22.02 GPa	50.86 GPa
$v_{m\ (0.5\ MPa)}$	Mean	0.32	0.07	0.18	0.47
$E_{m\ (32\ MPa)}$	High	50.48 GPa	2.35 GPa	46.29 GPa	54.01 GPa
$v_{m\ (32\ MPa)}$	High	0.26	0.01	0.26	0.27
$E_{m\ (8\ MPa)}$	High	48.63 GPa	2.61 GPa	44.20 GPa	52.59 GPa
$v_{m\ (8\ MPa)}$	High	0.27	0.01	0.25	0.29
$E_{m\ (0.5\ MPa)}$	High	33.6 GPa	8.25 GPa	22.02 GPa	50.59 GPa
$v_{m\ (0.5\ MPa)}$	High	0.37	0.07	0.23	0.45

Table 4-3. DFN geometry-induced variability in rock mass strength properties of Rock Domain RSMA01.

Variable	P32	Mean	Std. Dev.	Min.	Max.
GSI	Low	84	5	76	91
m_i	Low	25	4.6	14	31
σ_t H&B	Low	–2.63 MPa	1.49	–6.04 MPa	–1.13 MPa
σ_c H&B	Low	80.74 MPa	23.44	51.0 MPa	117.6 MPa
c_m MC	Low	17.82 MPa	4.11	10.75 MPa	23.69 MPa
φ_m MC	Low	49.88	1.72	44.43	52.19
GSI	Mean	69	5	61	77
m_i	Mean	27	2.7	23	34
σ_t H&B	Mean	–0.73 MPa	0.3	–1.43 MPa	–0.38 MPa
σ_c H&B	Mean	35.08 MPa	9.20	21.96 MPa	53.93 MPa
c_m MC	Mean	12.93 MPa	0.91	11.40 MPa	14.57 MPa
φ_m MC	Mean	48.13	1.22	45.86	50.09
GSI	High	65	6	49	76
m_i	High	27	2.3	22	32
σ_t H&B	High	–0.56 MPa	0.24	–1.27 MPa	–0.16 MPa
σ_c H&B	High	28.48 MPa	8.46	11.01 MPa	51.00 MPa
c_m MC	High	12.11 MPa	1.02	9.56 MPa	14.37 MPa
φ_m MC	High	46.84	1.73	41.99	49.82

4.3 Summary of DFN geometry-induced rock mass variability

In Figure 4-3 and Figure 4-4 the evaluated deformation modulus and Poisson's ratio from all the 3DEC simulations on DFN-realisations for rock domain RSMA01 are shown as a function of the confining pressure.

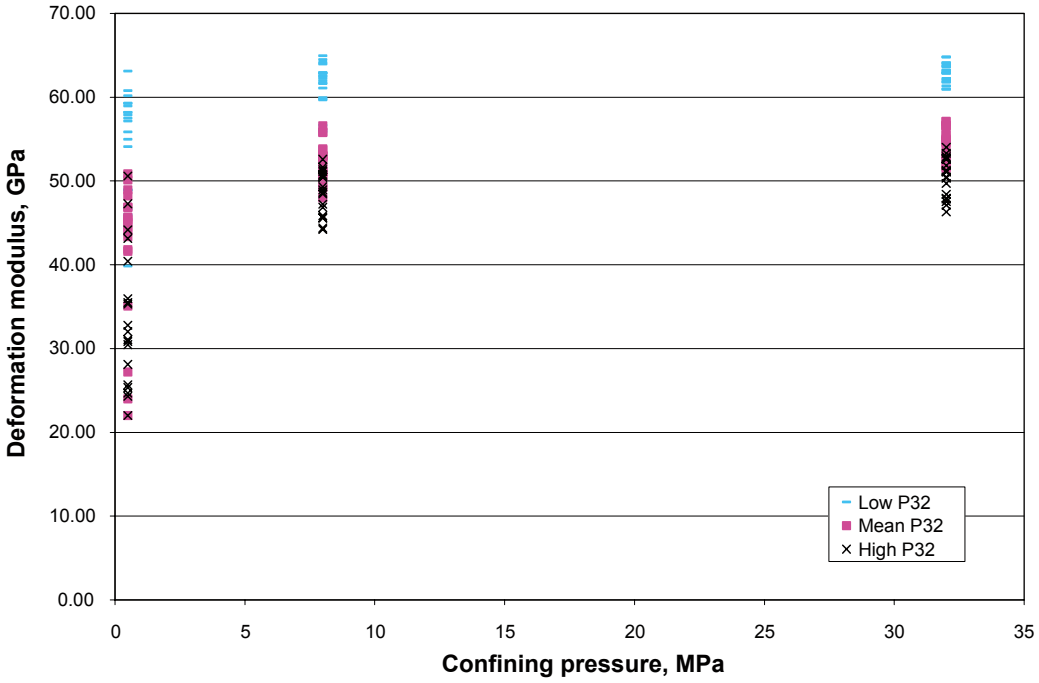

Figure 4-3. *Variation of deformation modulus with confining pressure for all DFN realisations.*

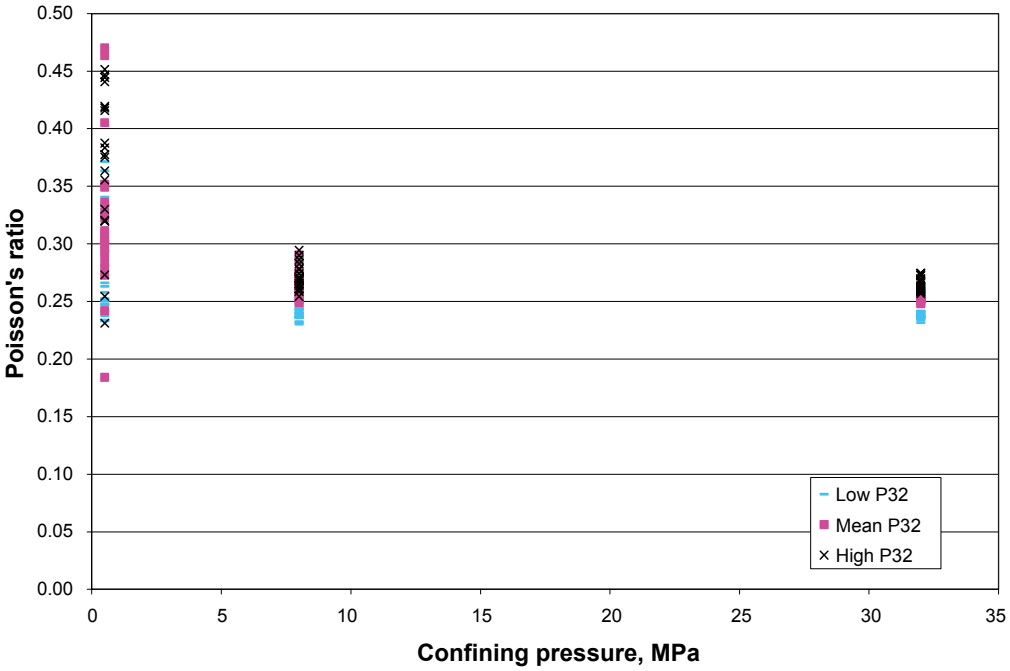

Figure 4-4. *Variation of Poisson's ratio with confining pressure for all DFN realisations.*

In Figure 4-5 to Figure 4-7 the evaluated deformation modulus is plotted against the fracture intensity P_{10} for each realisation and confining pressure. In Figure 4-8 to Figure 4-10 the evaluated Poisson's ratio is plotted against the fracture intensity P_{10} for each realisation and confining pressure.

A clear variation with P_{10} is shown in the plots.

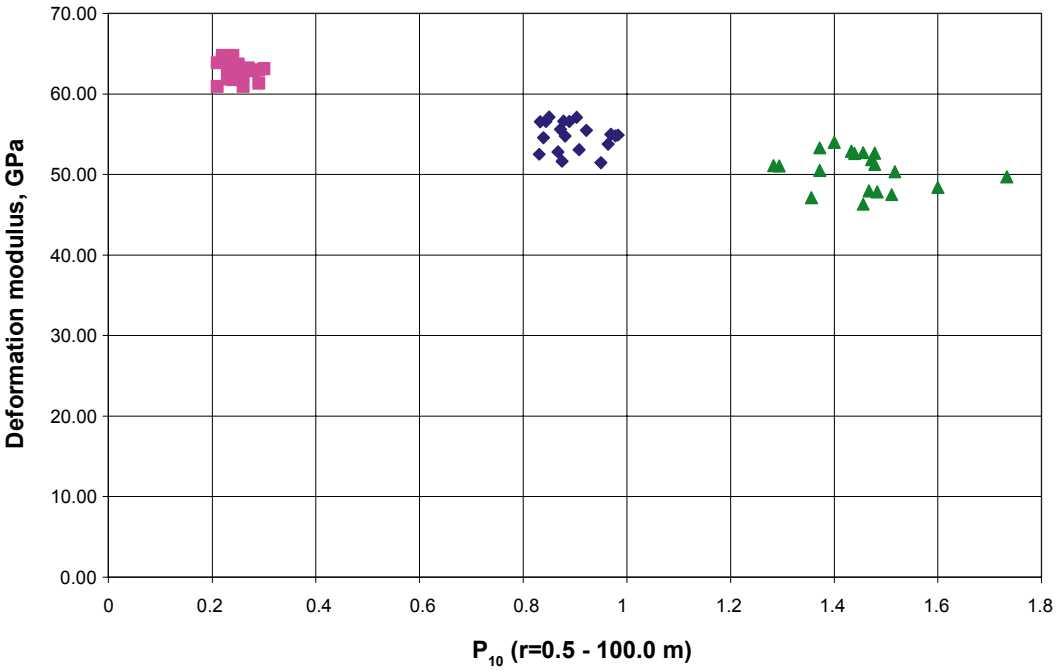

Figure 4-5. *The variation of deformation modulus with P_{10} at stress level 32 MPa.*

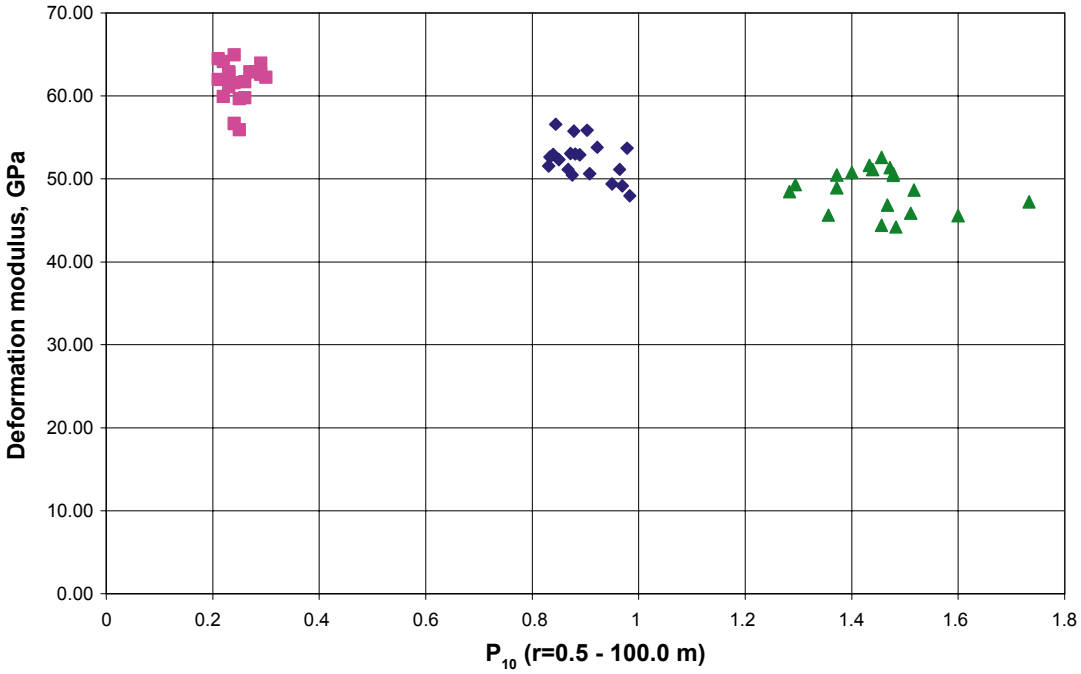

Figure 4-6. *The variation of deformation modulus with P_{10} at stress level 8 MPa.*

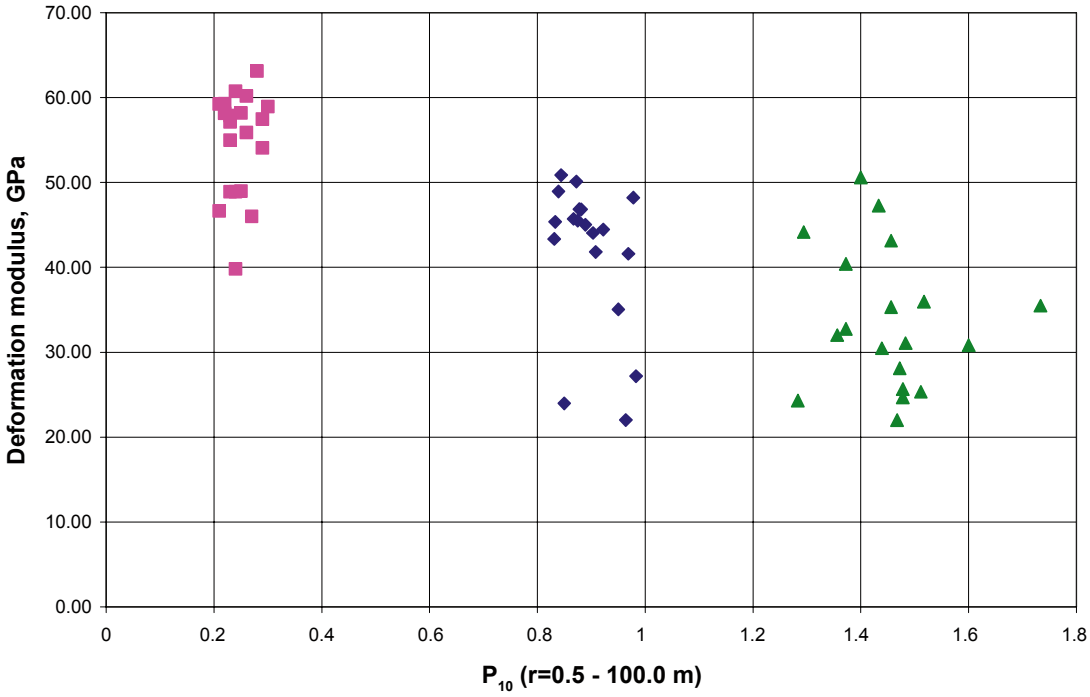

Figure 4-7. *The variation of deformation modulus with P_{10} at stress level 0.5 MPa.*

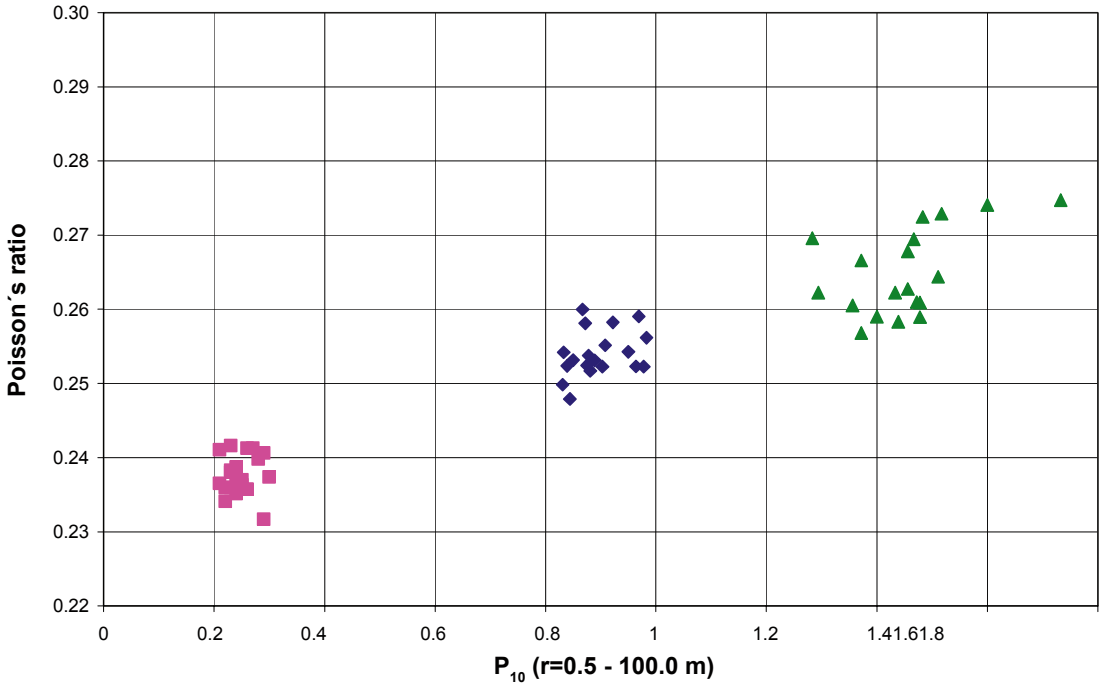

Figure 4-8. *The variation of Poisson's ratio with P_{10} at stress level 32 MPa.*

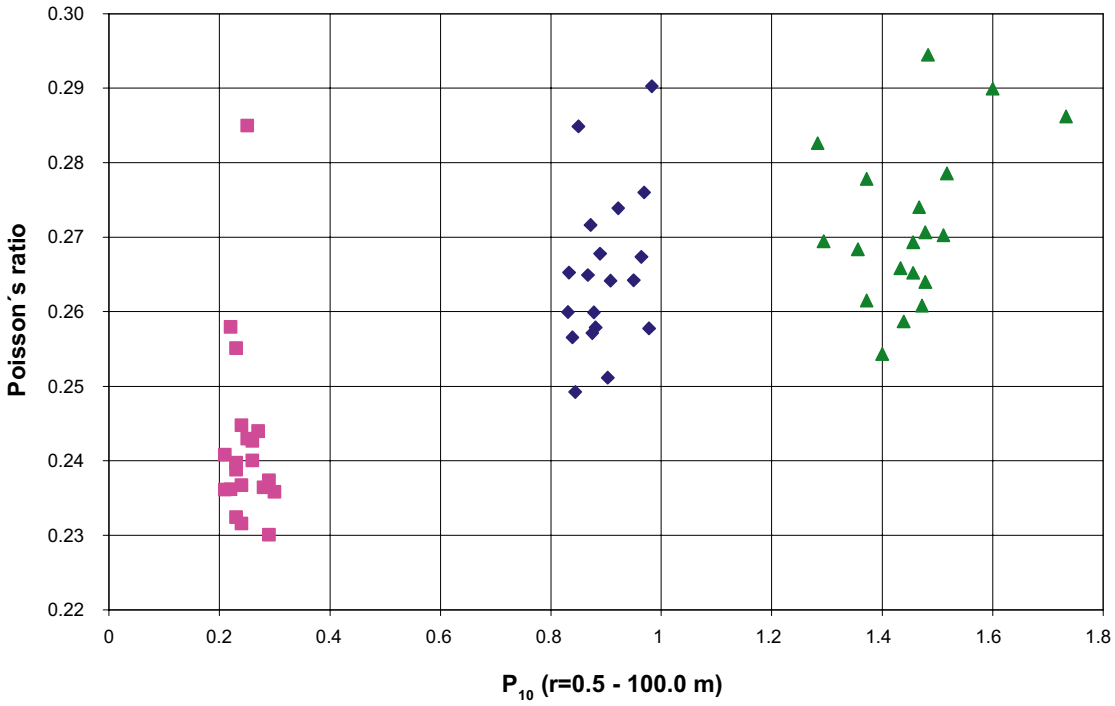

Figure 4-9. *The variation of Poisson's ratio with P_{10} at stress level 8 MPa.*

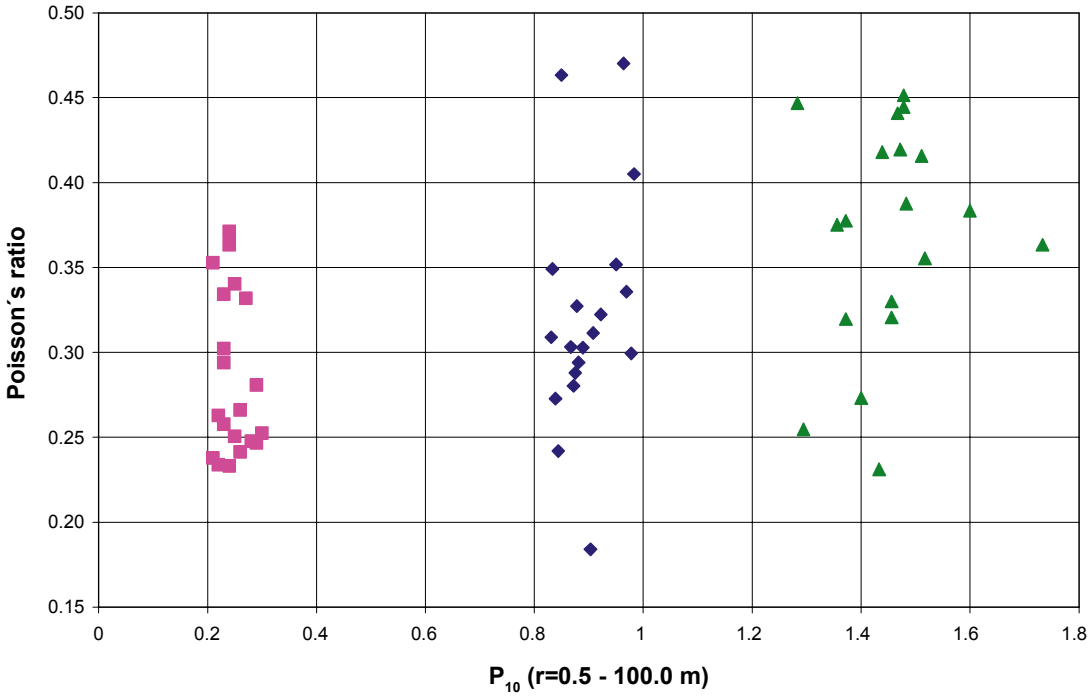

Figure 4-10. *The variation of Poisson's Ratio with P_{10} at stress level 0.5 MPa.*

In Figure 4-11 and Figure 4-12 the evaluated friction angle φ_m and cohesion c_m according to Mohr-Coulomb are shown as a function of P_{10}.

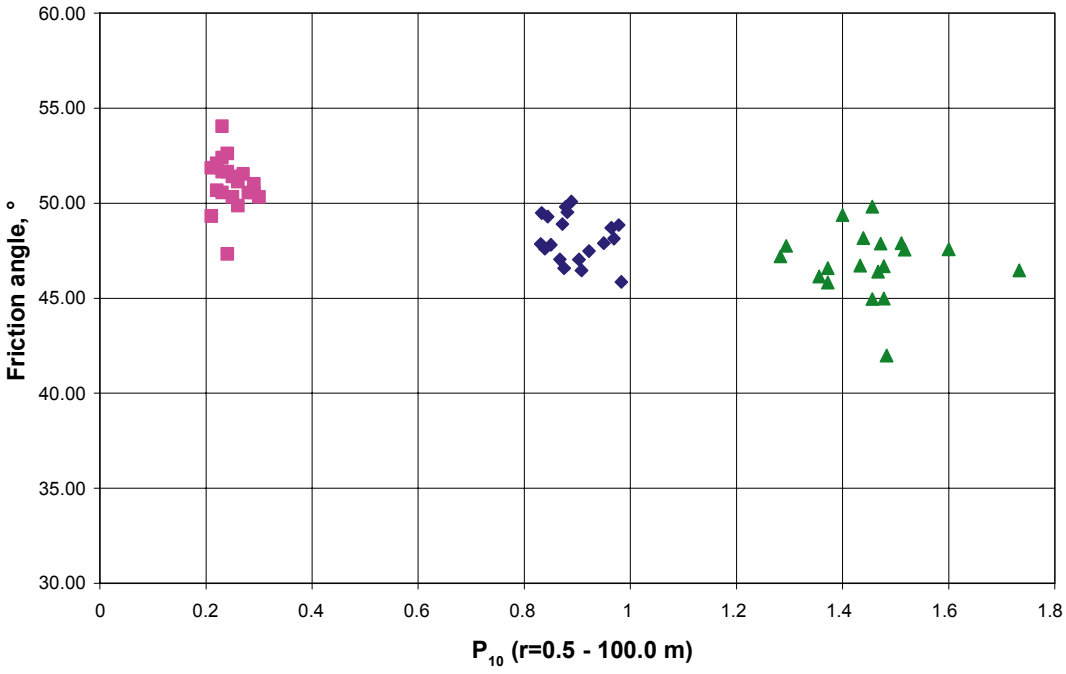

Figure 4-11. *The variation of the friction angle according to Mohr-Coulomb with P_{10}.*

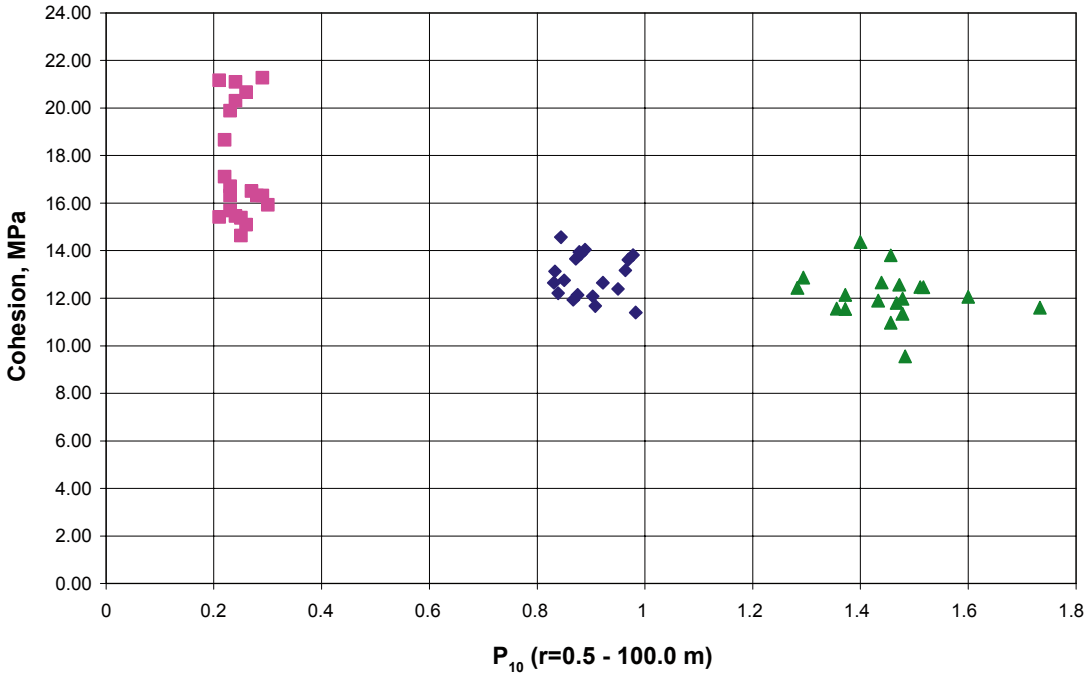

Figure 4-12. *The variation of the cohesion according to Mohr-Coulomb with P_{10}.*

In Figure 4-13 to Figure 4-15 the evaluated parameters GSI, uniaxial compressive strength σ_c and the tensile strength σ_t of the rock mass according to Hoek-Brown criterion are shown as a function of P_{10}.

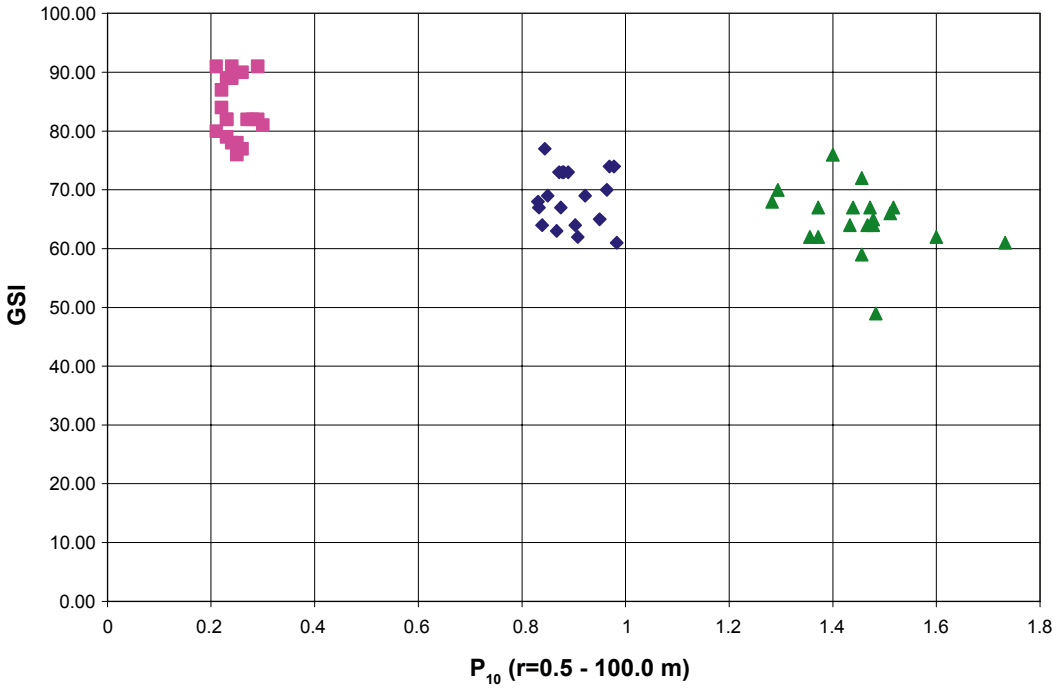

Figure 4-13. *The variation of GSI with P_{10}.*

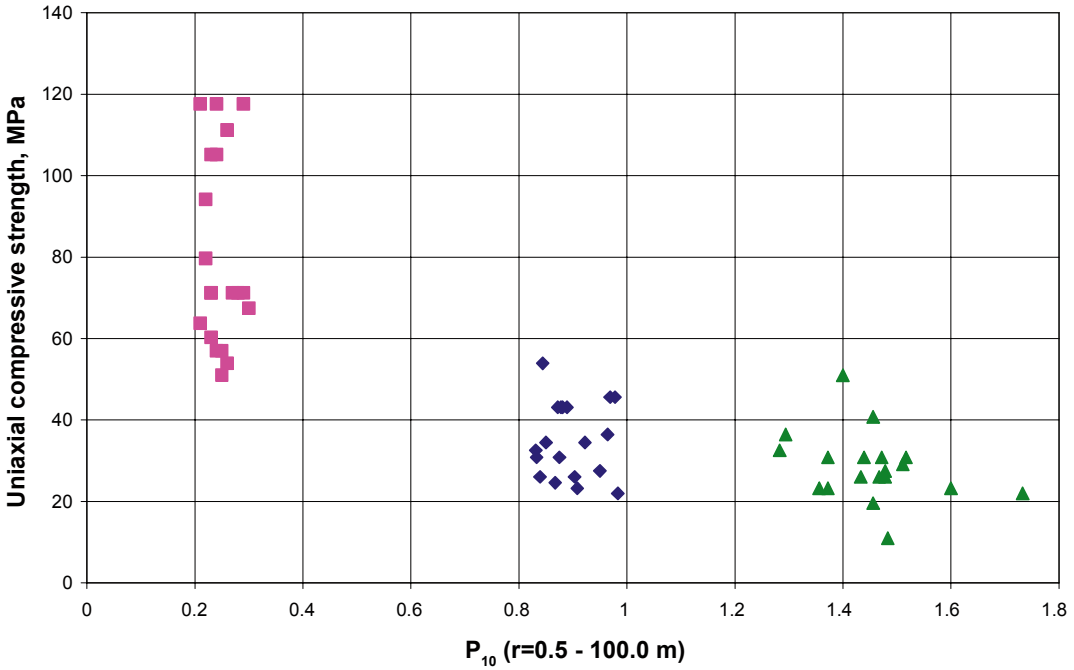

Figure 4-14. *The variation of the uniaxial compressive strength according to Hoek & Brown with P_{10}.*

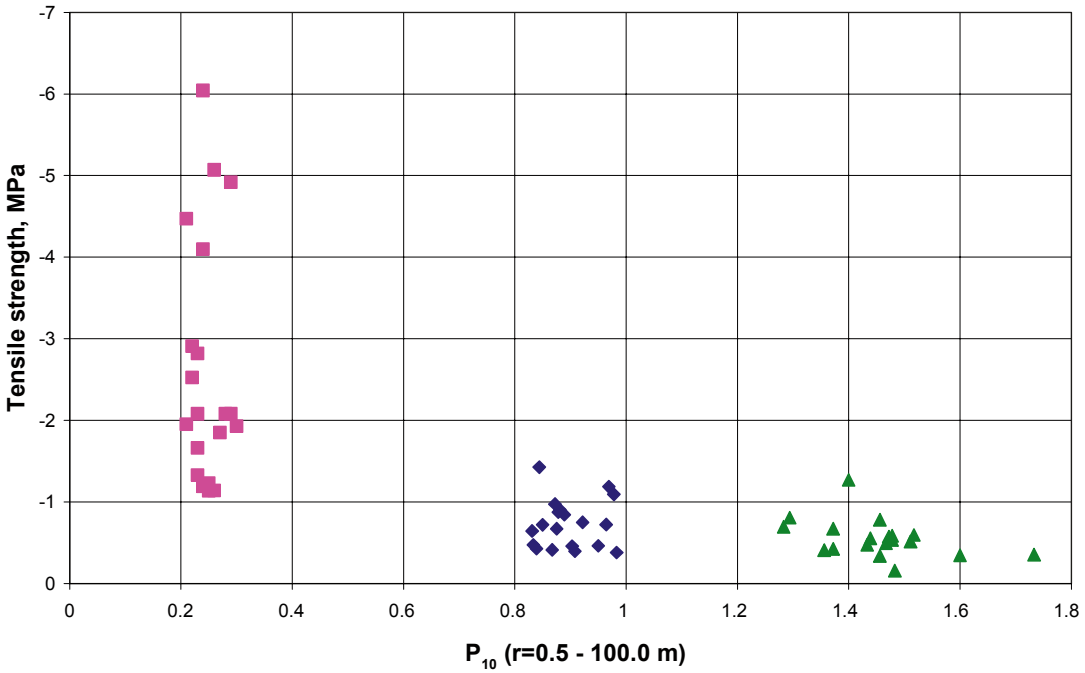

Figure 4-15. *The variation of the tensile strength according to Hoek & Brown with P_{10}.*

5 Discussions and conclusions

It should be emphasised that the fracture geometry parameterisation used in this study was taken from the best available understanding at the time: The Laxemar DFN model version 1.2, presented the 20th April 2005 and reported in /Hermanson et al. 2005/. Since that time, the parameters of the DFN model have been re-evaluated, which has lead to some adjustments (particularly in fracture intensities of sets S_A, S_B, and S_C). These adjustments may have impacts on the mechanical properties of the rock mass, although it is currently difficult to speculate on the full extent of these changes.

The influence of fracture intensity has been studied in more detail compared with the previous model for the Simpevarp subarea /Fredriksson and Olofsson 2005/. Moreover the rock block has been confined at three different levels down to 0.5 MPa. The fracture intensity but also the confining stress has a great influence on the deformation properties (E_m, ν_m) of the rock mass. Also the strength properties are clearly influenced by the fracture intensity. By varying the confining stress it was possible to fit the non-linear Hoek-Brown criterion to the results of the numerical simulations.

- The evaluated parameters are valid for an effective confining stress range from 0.5 MPa to 32 MPa. This stress interval has been chosen to catch the estimated in situ stresses in both stress domains from the surface down to 500 m depth.
- Variation in fracture properties between different fracture sets in DFN realisations have not been examined, because the laboratory tests on fracture samples do not show any significant difference between the fracture sets. Hence, all fractures within a DFN realisation have been assigned the same values.
- The DFN-induced variability component is only evaluated for a limited number of realisations for each set up of DFN-parameters, i.e. 20 realisations. The P_{32} has been varied from a low value (P_{32} mean – Std. dev.) to a high value (P_{32} mean + Std. dev.).
- The rock mass deformation properties are affected by the fracture intensity. Distinct trends can be identified for deformation modulus and Poisson's ratio towards P_{10} at 8 and 32 MPa confining stress. At 0.5 MPa confining stress the variability at each P_{32} case is much higher and the trends are farther less distinct. The deformation modulus decreases with increasing P_{32} whereas the Poisson's ratio increases.
- The rock mass strength properties are also affected by the fracture intensity. Quite distinct trends can be established for all the parameters. Friction angle, cohesion, GSI,, Uniaxial compressive strength and tensile strength decrease with increasing P_{32}. The variations are not significant for values at 8 and 32 MPa confining stress.

The resulting rock mass mechanical properties and their variation are presented in Table 5-1 to Table 5-9 for the three alternative DFN models. Only the value of P_{32} differs between the models. These tables illustrate clearly the influence of the P_{32} on the rock mechanical properties, especially on the deformation modulus and uniaxial compressive strength. These parameters are significantly affected by an increase in fracture density in the model.

The results of the theoretical approach shall be harmonized with the empirical approach before the design values of the material properties of the rock mass are determined.

Table 5-1. Deformation modulus at stress level 32 MPa.

$E_{m(32\ MPa)}$ [GPa]	P_{32} low	P_{32} mean	P_{32} high
Mean	62.90	54.78	50.48
Standard dev.	1.17	1.81	2.35
Min.	60.92	51.47	46.29
Max	64.80	57.13	54.01

Table 5-2. Deformation modulus at stress level 8 MPa.

$E_{m(8\ MPa)}$ [GPa]	P_{32} low	P_{32} mean	P_{32} high
Mean	61.73	52.31	48.63
Standard dev.	2.37	2.31	2.61
Min.	55.91	47.97	44.20
Max	64.94	56.97	52.59

Table 5-3. Deformation modulus at stress level 0.5 MPa.

$E_{m(0.5\ MPa)}$ [GPa]	P_{32} low	P_{32} mean	P_{32} high
Mean	54.73	41.94	33.87
Standard dev.	6.11	8.59	8.25
Min.	39.83	22.02	22.02
Max	63.12	50.86	50.59

Table 5-4. Poisson's ratio at stress level 32 MPa.

$v_{m(32\ MPa)}$	P_{32} low	P_{32} mean	P_{32} high
Mean	0.24	0.25	0.26
Standard dev.	0.003	0.003	0.01
Min.	0.23	0.25	0.26
Max	0.24	0.26	0.27

Table 5-5. Poisson's ratio at stress level 8 MPa.

$v_{m(8\ MPa)}$	P_{32} low	P_{32} mean	P_{32} high
Mean	0.24	0.27	0.27
Standard dev.	0.10	0.01	0.01
Min.	0.23	0.25	0.25
Max	0.28	0.29	0.29

Table 5-6. Poisson's ratio at stress level 0.5 MPa.

$\nu_{mL(0.5\ MPa)}$	P_{32} low	P_{32} mean	P_{32} high
Mean	0.29	0.32	0.37
Standard dev.	0.05	0.07	0.07
Min.	0.23	0.18	0.23
Max	0.37	0.47	0.45

Table 5-7. Friction angle of the rock mass according to Mohr-Coulomb.

φ_m [°]	P_{32} low	P_{32} mean	P_{32} high
Mean	49.88	48.13	46.84
Standard dev.	1.72	1.22	1.73
Min.	44.43	45.86	41.99
Max	52.19	50.09	49.82

Table 5-8. Cohesion of the rock mass according to Mohr-Coulomb.

c_m [MPa]	P_{32} low	P_{32} mean	P_{32} high
Mean	17.82	12.93	12.11
Standard dev.	4.11	0.91	1.02
Min.	10.75	11.40	9.56
Max	23.69	14.57	14.37
Correlation between ϕ_m and c_m	0.106	0.915	0.963

Table 5-9. The uniaxial compressive strength of the rock mass, UCS_m, based on Mohr – Coulomb (Equation 2.2).

UCS_m [MPa]	P_{32} low	P_{32} mean	P_{32} high
Mean	99.1	67.8	61.5
Standard dev.	14.4	6.8	7.7
Min.	88.1	56.2	42.9
Max	124.8	78.6	77.6

6 References

Hermanson J, Forssberg O, Aaron F, La Pointe P, 2005. Statistical model of fractures and deformation zones. Preliminary site description, Laxemar subarea, version 1.2. SKB R-05-45, Svensk kärnbränslehantering AB.

Fredriksson A, Olofsson I, 2005. Rock mechanics characterisation of the rock mass – Theoretical approach, preliminary site description. Simpevarp subarea – version 1.2. SKB R-05-87, Svensk Kärnbränslehantering AB.

Hakami E, Min K-B, 2005. Modelling of the state of stress. Preliminary site description, Simpevarp subarea – version 1.2. SKB R-05-19. Svensk Kärnbränslehantering AB.

Lanaro F, Öhman J, Fredriksson A, 2006. Rock mechanics modeling of rock mass properties – Summary of the primary data, preliminary site description, Laxemar subarea – version 1.2. SKB R-06-15, Svensk Kärnbränslehantering AB.

Olofsson I, Fredriksson A, 2005. Strategy for a numerical Rock Mechanics Site Descriptive Model. Further development of the theoretical approach. SKB R-05-43. Svensk Kärnbränslehantering AB.

RocData User's guide, 2004. Strength analysis of rock and soil masses using the generalized Hoek-Brown, Mohr-Coulomb, Barton-Bandis and Power Curve failure criteria. Rocscience Inc.

Appendix A

Table A-1. Poisson's ratio, deformation modulus and vertical stress at failure for all DFN realisations, stress level 32 MPa and low P_{32}.

DFN realisation	P_{10}	Poisson's ratio, v_m	Deformation modulus, E_m, GPa	Vertical stress at failure, σ_{vf}, MPa
1	0.25	0.24	63.65	305.28
2	0.23	0.24	62.86	354.62
3	0.25	0.24	63.69	327.30
4	0.22	0.23	64.10	355.15
5	0.26	0.24	60.94	332.62
6	0.24	0.24	61.77	290.88
7	0.23	0.24	61.85	333.30
8	0.21	0.24	60.92	299.25
9	0.24	0.24	62.08	335.44
10	0.23	0.24	62.83	321.02
11	0.27	0.24	63.23	338.90
12	0.23	0.24	64.11	402.42
13	0.26	0.24	62.22	326.02
14	0.21	0.24	63.87	367.44
15	0.28	0.24	62.88	322.08
16	0.29	0.24	62.99	321.74
17	0.22	0.24	64.77	323.75
18	0.29	0.23	61.33	351.88
19	0.24	0.24	64.80	381.35
20	0.3	0.24	63.15	315.92
Mean	**0.25**	**0.24**	**62.90**	**335.32**
Standard dev.	**0.03**	**0.003**	**1.17**	**27.26**
Min.	**0.21**	**0.23**	**60.92**	**290.88**
Max	**0.30**	**0.24**	**64.80**	**402.42**

Table A-2. Poisson's ratio, deformation modulus and vertical stress at failure for all DFN realisations, stress level 8.0 MPa and low P_{32}.

DFN realisation	P_{10}	Poisson's ratio, v_m	Deformation modulus, E_m, GPa	Vertical stress at failure, σ_{vf}, MPa
1	0.25	0.24	59.66	138.26
2	0.23	0.26	61.09	173.88
3	0.25	0.28	55.91	161.15
4	0.22	0.26	59.94	182.30
5	0.26	0.24	59.78	192.59
6	0.24	0.24	56.67	171.78
7	0.23	0.24	62.44	168.07
8	0.21	0.24	61.98	143.30
9	0.24	0.24	61.61	155.93
10	0.23	0.24	62.89	167.24
11	0.27	0.24	62.92	178.82
12	0.23	0.23	62.84	208.71
13	0.26	0.24	61.71	139.27
14	0.21	0.24	64.49	199.89
15	0.28	0.24	62.91	157.74
16	0.29	0.24	63.94	152.55
17	0.22	0.24	64.13	173.75
18	0.29	0.23	62.56	199.76
19	0.24	0.23	64.94	204.92
20	0.3	0.24	62.24	163.07
Mean	**0.25**	**0.24**	**61.73**	**171.65**
Standard dev.	**0.03**	**0.01**	**2.37**	**21.36**
Min.	**0.21**	**0.23**	**55.91**	**138.26**
Max	**0.30**	**0.28**	**64.94**	**208.71**

Table A-3. Poisson's ratio, deformation modulus and vertical stress at failure for all DFN realisations, stress level 0.5 MPa and low P_{32}.

DFN realisation	P_{10}	Poisson's ratio, ν_m	Deformation modulus, E_m, GPa	Vertical stress at failure, σ_{vf}, MPa
1	0.25	0.25	58.19	71.56
2	0.23	0.30	57.14	88.90
3	0.25	0.34	48.98	83.21
4	0.22	0.26	58.16	108.66
5	0.26	0.24	55.87	107.81
6	0.24	0.37	39.83	105.21
7	0.23	0.29	54.97	71.13
8	0.21	0.35	46.64	54.94
9	0.24	0.36	48.90	72.89
10	0.23	0.33	48.91	87.12
11	0.27	0.33	46.01	81.94
12	0.23	0.26	57.86	129.24
13	0.26	0.27	60.17	58.14
14	0.21	0.24	59.24	122.04
15	0.28	0.25	63.12	76.29
16	0.29	0.28	54.08	72.90
17	0.22	0.23	59.28	96.88
18	0.29	0.25	57.48	117.56
19	0.24	0.23	60.77	115.72
20	0.3	0.25	58.95	88.25
Mean	**0.25**	**0.29**	**54.73**	**90.52**
Standard dev.	**0.03**	**0.05**	**6.11**	**21.48**
Min.	**0.21**	**0.23**	**39.83**	**54.94**
Max	**0.30**	**0.37**	**63.12**	**129.24**

Table A-4. Friction angle (MC), cohesion (MC), GSI, m_i, tensile strength, σ_t (H&B) and uniaxial compressive strength, σ_c (H&B) for the rock mass at low P_{32}.

DFN realisation	Friction angle, ° Mohr-Coulomb	Cohesion, MPa Mohr-Coulomb	GSI	m_i	σ_t, MPa Hoek & Brown	σ_c, MPa Hoek & Brown
1	50.32	14.63	76.00	28	–1.1338	50.997
2	52.41	16.71	82.00	30	–1.6636	71.262
3	51.40	15.38	78.00	30	–1.2305	57.02
4	52.09	18.66	87.00	25	–2.91	94.132
5	49.87	20.66	90.00	18	–5.07	111.2
6	47.33	20.30	89.00	14	–6.0431	105.209
7	51.66	15.69	79.00	30	–1.3269	60.29
8	49.33	15.41	80.00	22	–1.951	63.747
9	51.67	15.46	78.00	31	–1.1908	57.019
10	50.56	16.31	82.00	24	–2.0795	71.262
11	51.55	16.51	82.00	27	–1.8485	71.262
12	54.05	19.88	89.00	30	–2.8201	105.209
13	51.14	15.09	77.00	30	–1.1411	53.925
14	51.86	21.17	91.00	22	–4.4715	117.59
15	50.56	16.31	82.00	24	–2.0795	71.26
16	50.56	16.31	82.00	24	–2.0795	71.26
17	50.69	17.11	84.00	23	–2.5231	79.657
18	51.02	21.28	91.00	20	–4.9197	117.586
19	52.62	21.10	91.00	24	–4.0989	117.586
20	50.32	15.93	81.00	24	–1.9285	67.4
Mean	**51.05**	**17.49**	**83.55**	**25.00**	**–2.63**	**80.74**
Standard dev.	**1.38**	**2.34**	**5.09**	**4.57**	**1.49**	**23.44**
Min.	**47.33**	**14.63**	**76.00**	**14.00**	**–6.04**	**51.00**
Max	**54.05**	**21.28**	**91.00**	**31.00**	**–1.13**	**117.59**

Appendix B

Table B-1. Poisson's ratio, deformation modulus and vertical stress at failure for all DFN realisations, stress level 32.0 MPa and mean P_{32}.

DFN realisation	P_{10}	Poisson's ratio, v_m	Deformation modulus, E_m, GPa	Vertical stress at failure, σ_{vf}, MPa
1	0.964	0.25	53.77	279.46
2	0.889	0.25	56.57	303.52
3	0.875	0.25	51.63	247.26
4	0.969	0.26	54.98	273.32
5	0.983	0.26	54.89	235.02
6	0.85	0.25	57.13	265.75
7	0.881	0.25	54.76	291.60
8	0.903	0.25	57.09	250.32
9	0.908	0.26	53.07	243.54
10	0.867	0.26	52.80	252.83
11	0.978	0.25	54.80	286.06
12	0.878	0.25	56.63	294.34
13	0.95	0.25	51.47	262.34
14	0.922	0.26	55.47	260.09
15	0.833	0.25	56.55	290.94
17	0.839	0.25	54.56	262.66
18	0.872	0.26	55.60	287.63
19	0.844	0.25	56.59	295.15
20	0.831	0.25	52.52	264.02
Mean	**0.90**	**0.25**	**54.78**	**270.83**
Standard dev.	**0.05**	**0.003**	**1.81**	**20.13**
Min.	**0.83**	**0.25**	**51.47**	**235.02**
Max	**0.98**	**0.26**	**57.13**	**303.52**

Table B-2. Poisson's ratio, deformation modulus and vertical stress at failure for all DFN realisations, stress level 8.0 MPa and mean P_{32}.

DFN realisation	P_{10}	Poisson's ratio, v_m	Deformation modulus, E_m, GPa	Vertical stress at failure, σ_{vf}, MPa
1	0.964	0.27	51.14	121.79
2	0.889	0.27	52.91	132.59
3	0.875	0.26	50.46	96.68
4	0.969	0.28	49.15	113.02
5	0.983	0.29	47.97	99.34
6	0.85	0.28	52.33	120.88
7	0.881	0.26	52.99	110.93
8	0.903	0.25	55.85	94.49
9	0.908	0.26	50.60	112.89
10	0.867	0.26	51.14	100.69
11	0.978	0.26	53.70	117.49
12	0.878	0.26	55.77	128.33
13	0.95	0.26	49.37	100.09
14	0.922	0.27	53.81	106.42
15	0.833	0.27	52.65	125.17
17	0.839	0.26	52.95	96.27
18	0.872	0.27	53.05	118.93
19	0.844	0.25	56.57	142.60
20	0.831	0.26	51.54	107.82
Mean	**0.90**	**0.27**	**52.31**	**112.97**
Standard dev.	**0.05**	**0.01**	**2.31**	**13.55**
Min.	**0.83**	**0.25**	**47.97**	**94.49**
Max	**0.98**	**0.29**	**56.57**	**142.60**

Table B-3. Poisson's ratio, deformation modulus and vertical stress at failure for all DFN realisations, stress level 0.5 MPa and mean P_{32}.

DFN realisation	P_{10}	Poisson's ratio, v_m	Deformation modulus, E_m, GPa	Vertical stress at failure, σ_{vf}, MPa
1	0.964	0.47	22.02	42.36
2	0.889	0.30	45.03	40.67
3	0.875	0.29	45.50	32.97
4	0.969	0.34	41.60	48.05
5	0.983	0.41	27.19	42.62
6	0.85	0.46	23.99	47.84
7	0.881	0.29	46.84	38.29
8	0.903	0.18	44.04	37.03
9	0.908	0.31	41.81	33.47
10	0.867	0.30	45.70	28.69
11	0.978	0.30	48.20	56.39
12	0.878	0.33	46.85	47.43
13	0.95	0.35	35.06	34.16
14	0.922	0.32	44.45	36.53
15	0.833	0.35	45.37	60.30
17	0.839	0.27	48.94	32.75
18	0.872	0.28	50.10	39.85
19	0.844	0.24	50.86	70.93
20	0.831	0.31	43.35	27.64
Mean	**0.90**	**0.32**	**41.94**	**42.00**
Standard dev.	**0.05**	**0.07**	**8.59**	**11.15**
Min.	**0.83**	**0.18**	**22.02**	**27.64**
Max	**0.98**	**0.47**	**50.86**	**70.93**

Table B-4. Friction angle (MC), cohesion (MC), GSI, m_i, tensile strength, σ_t (H&B) and uniaxial compressive strength, σ_c (H&B) for the rock mass at mean P_{32}.

DFN realisation	Friction angle, ° Mohr-Coulomb	Cohesion, MPa Mohr-Coulomb	GSI	m_i	σ_t, MPa Hoek & Brown	σ_c, MPa Hoek & Brown
1	48.70	13.17	70.00	28	–0.7213	36.458
2	50.09	14.04	73.00	30	–0.844	43.126
3	46.58	12.14	67.00	24	–0.6711	30.808
4	48.14	13.62	74.00	23	–1.1871	45.606
5	45.86	11.40	61.00	27	–0.3795	21.96
6	47.81	12.76	69.00	26	–0.7203	34.47
7	49.52	13.86	73.00	28	–0.9043	43.126
8	47.03	12.08	64.00	28	–0.4588	26.019
9	46.46	11.67	62.00	28	–0.3946	23.239
10	47.04	11.94	63.00	29	–0.4108	24.591
11	48.85	13.82	74.00	25	–1.0922	45.606
12	49.81	13.95	73.00	29	–0.8731	43.126
13	47.89	12.39	65.00	30	–0.4617	27.528
14	47.48	12.65	69.00	25	–0.7491	34.47
15	49.48	13.13	67.00	34	–0.4737	30.808
17	47.61	12.21	64.00	30	–0.4282	26.016
18	48.90	13.66	73.00	26	–0.9739	43.126
19	49.30	14.57	77.00	24	–1.4264	53.925
20	47.85	12.66	68.00	27	–0.6433	32.588
Mean	**48.13**	**12.93**	**68.74**	**27.42**	**–0.73**	**35.08**
Standard dev.	**1.22**	**0.91**	**4.72**	**2.67**	**0.30**	**9.20**
Min.	**45.86**	**11.40**	**61.00**	**23.00**	**–1.43**	**21.96**
Max	**50.09**	**14.57**	**77.00**	**34.00**	**–0.38**	**53.93**

Appendix C

Table C-1. Poisson's ratio, deformation modulus and vertical stress at failure for all DFN realisations, stress level 32 MPa and high P_{32}.

DFN realisation	P_{10}	Poisson's ratio, v_m	Deformation modulus, E_m, GPa	Vertical stress at failure, σ_{vf}, MPa
1	1.283	0.27	51.09	254.58
2	1.372	0.26	53.29	246.47
3	1.478	0.26	52.65	226.85
4	1.511	0.26	47.51	266.09
5	1.439	0.26	52.59	268.83
6	1.456	0.26	52.71	297.41
7	1.478	0.26	51.25	246.55
8	1.472	0.26	51.86	264.59
9	1.467	0.27	47.93	244.84
10	1.456	0.27	46.29	227.42
11	1.356	0.26	47.12	238.54
12	1.433	0.26	52.89	250.15
13	1.483	0.27	47.84	193.05
14	1.372	0.27	50.48	236.87
15	1.6	0.27	48.40	259.66
16	1.517	0.27	50.35	260.69
17	1.294	0.26	51.08	266.46
18	1.733	0.27	49.69	245.32
19	1.4	0.26	54.01	294.34
Mean	**1.45**	**0.26**	**50.48**	**252.04**
Standard dev.	**0.10**	**0.01**	**2.35**	**23.72**
Min.	**1.28**	**0.26**	**46.29**	**193.05**
Max	**1.73**	**0.27**	**54.01**	**297.41**

Table C-2. Poisson's ratio, deformation modulus and vertical stress at failure for all DFN realisations, stress level 8.0 MPa and high P_{32}.

DFN realisation	P_{10}	Poisson's ratio, v_m	Deformation modulus, E_m, GPa	Vertical stress at failure, σ_{vf}, MPa
1	1.283	0.28	48.45	92.30
2	1.372	0.26	50.47	89.58
3	1.478	0.26	50.44	78.49
4	1.511	0.27	45.84	102.16
5	1.439	0.26	51.12	104.99
6	1.456	0.27	52.59	120.19
7	1.478	0.27	50.64	86.63
8	1.472	0.26	51.35	99.53
9	1.467	0.27	46.85	83.74
10	1.456	0.27	44.39	79.08
11	1.356	0.27	45.63	95.09
12	1.433	0.27	51.62	101.41
13	1.483	0.29	44.20	75.75
14	1.372	0.28	48.93	82.77
15	1.6	0.29	45.57	90.80
16	1.517	0.28	48.65	96.11
17	1.294	0.27	49.30	119.53
18	1.733	0.29	47.22	87.88
19	1.4	0.25	50.77	117.89
Mean	**1.45**	**0.27**	**48.63**	**94.94**
Standard dev.	**0.10**	**0.01**	**2.61**	**13.59**
Min.	**1.28**	**0.25**	**44.20**	**75.75**
Max	**1.73**	**0.29**	**52.59**	**120.19**

Table C-3. Poisson's ratio, deformation modulus and vertical stress at failure for all DFN realisations, stress level 0.5 MPa and high P_{32}.

DFN realisation	P_{10}	Poisson's ratio, v_m	Deformation modulus, E_m, GPa	Vertical stress at failure, σ_{vf}, MPa
1	1.283	0.45	24.31	27.83
2	1.372	0.38	32.77	31.39
3	1.478	0.45	24.69	22.44
4	1.511	0.42	25.36	26.54
5	1.439	0.42	30.47	31.70
6	1.456	0.32	43.14	49.35
7	1.478	0.44	25.67	23.08
8	1.472	0.42	28.11	27.53
9	1.467	0.44	22.02	27.10
10	1.456	0.33	35.32	13.75
11	1.356	0.38	32.03	27.65
12	1.433	0.23	47.27	39.16
13	1.483	0.39	31.07	28.19
14	1.372	0.32	40.42	27.99
15	1.6	0.38	30.84	20.17
16	1.517	0.36	35.96	22.60
17	1.294	0.25	44.17	30.72
18	1.733	0.36	35.49	22.24
19	1.4	0.27	50.59	43.85
Mean	**1.45**	**0.37**	**33.67**	**28.59**
Standard dev.	**0.10**	**0.07**	**8.25**	**8.31**
Min.	**1.28**	**0.23**	**22.02**	**13.75**
Max	**1.73**	**0.45**	**50.59**	**49.35**

Table C-4. Friction angle (MC), cohesion (MC), GSI, m_i, tensile strength, σ_t (H&B) and uniaxial compressive strength, σ_c (H&B) for the rock mass at high P_{32}.

DFN realisation	Friction angle, ° Mohr-Coulomb	Cohesion, MPa Mohr-Coulomb	GSI	m_i	σ_t, MPa Hoek & Brown	σ_c, MPa Hoek & Brown
1	47.20	12.44	68.00	25	–0.6947	32.59
2	46.58	12.14	67.00	24	–0.6711	30.808
3	44.98	11.35	64.00	22	–0.5839	26.019
4	47.89	12.47	66.00	29	–0.5151	29.123
5	48.17	12.66	67.00	29	–0.5554	30.808
6	49.82	13.81	72.00	30	–0.7827	40.78
7	46.69	11.98	65.00	26	–0.5328	27.528
8	47.87	12.56	67.00	28	–0.5752	30.808
9	46.40	11.80	64.00	26	–0.4941	26.019
10	44.96	10.97	59.00	26	–0.3389	19.6
11	46.15	11.56	62.00	27	–0.4092	23.24
12	46.72	11.90	64.00	27	–0.4758	26.019
13	41.99	9.56	49.00	26	–0.1595	11.014
14	45.83	11.54	62.00	26	–0.4249	23.239
15	47.58	12.06	62.00	32	–0.3453	23.239
16	47.57	12.46	67.00	27	–0.5966	30.808
17	47.76	12.87	70.00	25	–0.8078	36.458
18	46.47	11.60	61.00	29	–0.3533	21.96
19	49.38	14.37	76.00	25	–1.2699	50.997
Mean	**46.84**	**12.11**	**64.84**	**26.79**	**–0.56**	**28.48**
Standard dev.	**1.73**	**1.02**	**5.57**	**2.32**	**0.24**	**8.46**
Min.	**41.99**	**9.56**	**49.00**	**22.00**	**–1.27**	**11.01**
Max	**49.82**	**14.37**	**76.00**	**32.00**	**–0.16**	**51.00**